Determination of the Global Resistive Stability of a High Temperature Tokamak Plasma via Asymptotic Matching

Richard Fitzpatrick
Institute for Fusion Studies
Department of Physics
University of Texas at Austin
Austin, TX 78712

The recently developed TOMUHAWC code is designed to investigate the global resistive stability of high temperature tokamak plasmas with realistic equilibria. The code solves (by means of adaptive-step integration) the linearized, Fourier transformed, marginally-stable (i.e., zero inertia), ideal-MHD equations everywhere in the plasma except in the immediate vicinity of the various rational magnetic flux-surfaces, where the equations are singular. The solutions thus obtained are matched asymptotically across the rational surfaces to determine the elements of the so-called stability matrix. This matrix is calculated for both tearing and twisting (i.e., interchange) parity modes. As an illustration of the use of the code to determine global resistive stability, the information from the $n = 1$ stability matrix, calculated for an up-down symmetric, fixed boundary, JET-like plasma equilibrium, is combined with a Glasser-Green-Johnson linear resistive layer model.

I. INTRODUCTION

As is well known, the determination of global resistive stability in a high temperature tokamak plasma can be reduced to an asymptotic matching problem.[1] The system is conveniently divided into two regions. In the "outer" region, which comprises most of the plasma, the perturbation is described by the linearized, marginally-stable (i.e., zero inertia), equations of ideal magnetohydrodynamics (MHD). However, these equations become singular on so-called "rational" magnetic flux-surfaces. In the "inner" region, which is strongly localized around the various rational surfaces, additional effects such as resistivity and inertia become important. The non-ideal layer solution in the vicinity of a given rational surface

can generally be separated into independent tearing and twisting (i.e., interchange) parity components.[2] Finally, simultaneous asymptotic matching of the layer solutions in the inner region to the ideal-MHD solution in the outer region yields a matrix tearing/twisting dispersion relation.[3–9]

There are two main techniques for numerically calculating the elements of the tearing/twisting stability matrix. The first employs a finite element method of solution.[4–6] The second reduces the problem to a set of coupled differential equations (in which the independent variable is a flux-surface label) that are solved by means of adaptive-step integration.[8–10] The latter method was previously implemented in the T7 code.[9,10] However, this code only takes into account the coupling of poloidal harmonics whose mode numbers differ by less than four. Unfortunately, such an approach can only be justified in a relatively large aspect-ratio, low beta, weakly shaped, plasma equilibrium. This paper describes a new code, called TOMUHAWC, which is similar to T7, except that there is no restriction on the allowed mode number difference between coupled poloidal harmonics, and, hence, on the type of plasma equilibrium.

II. DESCRIPTION OF TOMUHAWC CODE

The analysis underlying the TOMUHAWC code is set out in detail in Appendix A. In the following, all lengths are normalized to the major radius of the plasma magnetic axis, R_0, all magnetic field-strengths to the vacuum toroidal field-strength at the magnetic axis, B_0, and all plasma pressures to B_0^2/μ_0. TOMUHAWC employs a right-handed flux coordinate system, r, θ, ϕ. Here, r is a flux-surface label with dimensions of length which is such that $r = 0$ at the magnetic axis, and $r = a$ at the plasma boundary. Moreover, θ is a "straight" poloidal angle defined such that $\theta = 0$ on the inboard mid-plane. Finally, ϕ is the geometric toroidal angle. The Jacobian of the coordinate system is (see Sect. A 1)

$$(\nabla r \times \nabla\theta \cdot \nabla\phi)^{-1} = r\,R^2. \tag{1}$$

(Here, R, ϕ, Z is a conventional right-handed cylindrical coordinate system whose symmetry axis corresponds to the toroidal symmetry axis of the plasma.) The equilibrium magnetic field is written (see Sect. A 2)

$$\mathbf{B}(r,\theta) = \frac{r\,g}{q}\,\nabla(\phi - q\,\theta) \times \nabla r = \nabla\phi \times \nabla\Psi + g\,\nabla\phi, \tag{2}$$

where

$$\Psi(r) = -\int_r^a \frac{r\,g}{q}\,dr \tag{3}$$

is the poloidal magnetic flux, $q(r)$ the safety-factor profile, and $g(r)$ determines the toroidal magnetic field-strength.

The TOMUHAWC code requires the $q(r)$ and dq/dr profiles, as well as the following six profile functions (see Sect. A 4):

$$p_1(r) = r^2, \tag{4}$$

$$p_2(r) = \left(\frac{q}{g}\right)\frac{1}{r}\frac{dg}{dr} = \frac{dg}{d\Psi}, \tag{5}$$

$$p_3(r) = \left(\frac{q}{g}\right)^2\frac{1}{r}\frac{dP}{dr} = \frac{q}{g}\frac{dP}{d\Psi}, \tag{6}$$

$$p_4(r) = \left(\frac{q}{g}\right) r\,\frac{d}{dr}\left(\frac{g}{q}\right), \tag{7}$$

$$p_5(r) = \left(\frac{r\,g}{q}\right)^2 = \left(\frac{d\Psi}{dr}\right)^2, \tag{8}$$

$$p_6(r) = \Gamma\,P, \tag{9}$$

where $P(r)$ is the equilibrium plasma pressure, and $\Gamma = 5/3$ the plasma ratio of specific heats. (Note that p_1, p_2, p_3, p_4, and p_5 correspond to α_ϵ, α_g, α_p, α_f, and f^2, respectively, in Appendix A.) In addition, the code requires the following nine metric functions (see

Sect. A 4):

$$M^{(1)}_{jj'}(r) = \oint R^2 \, \exp\left[-\mathrm{i}\,(m_j - m_{j'})\,\theta\right] \frac{d\theta}{2\pi}, \tag{10}$$

$$M^{(2)}_{jj'}(r) = \oint |\nabla r|^{-2} \, R^{-2} \exp\left[-\mathrm{i}\,(m_j - m_{j'})\,\theta\right] \frac{d\theta}{2\pi}, \tag{11}$$

$$M^{(3)}_{jj'}(r) = \oint |\nabla r|^{-2} \exp\left[-\mathrm{i}\,(m - m')\,\theta\right] \frac{d\theta}{2\pi}, \tag{12}$$

$$M^{(4)}_{jj'}(r) = \oint |\nabla r|^{-2} \, R^2 \exp\left[-\mathrm{i}\,(m_j - m_{j'})\,\theta\right] \frac{d\theta}{2\pi}, \tag{13}$$

$$M^{(5)}_{jj'}(r) = \oint |\nabla r|^{-2} \, R^4 \exp\left[-\mathrm{i}\,(m_j - m_{j'})\,\theta\right] \frac{d\theta}{2\pi}, \tag{14}$$

$$M^{(6)}_{jj'}(r) = \oint \frac{\mathrm{i}\, r\, \nabla r \cdot \nabla\theta}{|\nabla r|^{\,2}} \exp\left[-\mathrm{i}\,(m_j - m_{j'})\,\theta\right] \frac{d\theta}{2\pi}, \tag{15}$$

$$M^{(7)}_{jj'}(r) = \oint \frac{\mathrm{i}\, r\, \nabla r \cdot \nabla\theta}{|\nabla r|^{\,2}} \, R^2 \exp\left[-\mathrm{i}\,(m_j - m_{j'})\,\theta\right] \frac{d\theta}{2\pi}, \tag{16}$$

$$M^{(8)}(r) = \oint |\nabla r|^{\,2} \frac{d\theta}{2\pi}, \tag{17}$$

$$M^{(9)}(r) = \oint R^4 \frac{d\theta}{2\pi}. \tag{18}$$

(Note that the $M^{(l)}_{jj'}$, for $l = 1, 7$, correspond to the $a_{jj'}$, $b_{jj'}$, $c_{jj'}$, $d_{jj'}$, $e_{jj'}$, $f_{jj'}$, and $g_{jj'}$, respectively, in Appendix A. Furthermore, $M^{(1)}_{00}$, $M^{(3)}_{00}$, $M^{(4)}_{00}$, $M^{(5)}_{00}$, $M^{(8)}$, and $M^{(9)}$ correspond to a_0, c_0, d_0, e_0, x_0, and y_0, respectively, in Appendix B.) Here, the m_j, where $j = 1, J$, are the mode numbers of the coupled poloidal harmonics included in the calculation. In principle, J can be made arbitrarily large. There is no restriction on the equilibrium other than the requirement that the profile functions, and their first derivatives, be finite and continuous. The same requirement applies to the metric functions.

The present version of TOMUHAWC assumes that the plasma is surrounded by a close fitting, perfectly conducting wall whose inner surface corresponds to the plasma boundary, $r = a$.

TOMUHAWC numerically integrates the linearized, Fourier transformed, marginally-stable, ideal-MHD equations, (A47)–(A48), in the region $0 \leq r \leq a$ using an explicit embedded Runge-Kutta Prince-Dormand method.[11] The solution is required to be well behaved at the magnetic axis, $r = 0$. The physical boundary condition $\delta\mathbf{B} \cdot \nabla r = 0$ is imposed at $r = a$. The linearized ideal-MHD equations are singular at plasma rational surfaces, which satisfy $q(r_k) = m_k/n$, for $k = 1, K$, where $0 \leq r_k \leq a$, Here, m_k is one of the m_j,

and n is the common toroidal mode number of the perturbation. The numerical solution in TOMUHAWC excludes the region of the plasma in which $|r - r_k| < \delta$, for $k = 1, K$, where $0 < \delta/a \ll 1$. The excluded region effectively constitutes the inner region, whereas the remainder of the plasma effectively constitutes the outer region. The solution also excludes the region close to the magnetic axis in which $r < \epsilon$, where $0 \leq \epsilon/a \ll 1$.

Writing

$$\delta\mathbf{B}\cdot\nabla r = \mathrm{i}\, R^{-2} \sum_{j=1,J} \frac{\psi_j(r)}{r}\, \exp[\,\mathrm{i}\,(m_j\,\theta - n\,\phi)], \tag{19}$$

the general analytic solution of the linearized ideal-MHD equations in the immediate vicinity of the kth rational surface is such that (see Sect. A 5)

$$\psi_k(r) = \Psi_k^{\pm}\, f_k\, |x_k|^{\nu_{L\,k}} + \Delta\Psi_k^{\pm}\, f_k\, \mathrm{sgn}(x_k)\, |x_k|^{\nu_{S\,k}} + A_k\, x_k + \cdots, \tag{20}$$

where

$$x_k = \left(\frac{r - r_k}{r_k}\right), \tag{21}$$

$$f_k = \left(\frac{m_k^2\, M^{(8)} + n^2\, p_1}{\nu_{S\,k} - \nu_{L\,k}}\right)^{1/2}_{r_k} = \left(\frac{m_k^2\, \langle|\nabla r|^{\,2}\rangle + n^2\, r^2}{2\,\sqrt{D_{I\,k}}}\right)^{1/2}_{r_k}, \tag{22}$$

and $\nu_{L\,k} = 1/2 - \sqrt{D_{I\,k}}$, $\nu_{S\,k} = 1/2 + \sqrt{D_{I\,k}}$. Here, $\langle\cdots\rangle = \oint(\cdots)\, d\theta/2\pi$ is a flux-surface average operator, and $D_{I\,k}$ a standard ideal interchange stability parameter evaluated at the surface [see Eq. (B42)].[2] Moreover, the plus superscript refers to the region $x_k > 0$, whereas the minus superscript refers to the region $x_k < 0$. The above analytic solution is asymptotically matched to the numerical solution at $r = r_k \pm \delta$. However, the matching process employed by TOMUHAWC is only valid provided $0 < D_{I\,k} < 1$. The process breaks down when $D_{I\,k} < 0$ because the plasma in the vicinity of the kth rational surface becomes unstable to localized ideal interchange modes.[12] The process breaks down when $D_{I\,k} > 1$ because the expansion (20) needs to be carried out to higher order in x_k.

It is helpful to define (see Sect. A 6)

$$\Psi_k^e = \frac{1}{2}\left(\Psi_k^+ + \Psi_k^-\right), \tag{23}$$

$$\Psi_k^o = \frac{1}{2}\left(\Psi_k^+ - \Psi_k^-\right), \tag{24}$$

$$\Delta\Psi_k^e = \Delta\Psi_k^+ + \Delta\Psi_k^-, \tag{25}$$

$$\Delta\Psi_k^o = \Delta\Psi_k^+ - \Delta\Psi_k^-. \tag{26}$$

The complex quantities Ψ_k^e and Ψ_k^o parameterize the amount of magnetic reconnection generated by tearing and twisting parity modes, respectively, at the kth rational surface. (Thus, in a zero-inertia ideal plasma, $\Psi_k^e = \Psi_k^o = 0$, for all k.) Moreover, the complex quantities

$$\Delta_k^e = \frac{\Delta\Psi_k^e}{\Psi_k^e}, \tag{27}$$

$$\Delta_k^o = \frac{\Delta\Psi_k^o}{\Psi_k^o}, \tag{28}$$

are completely determined by the tearing and twisting parity resistive layer solutions, respectively, in the vicinity of the kth rational surface (see Appendix B). When simultaneously applied to every rational surface in the plasma, the asymptotic matching process leads to a matrix dispersion relation of the form (see Sect. A 8)

$$\Delta_k^e\,\Psi_k^e = \Delta\Psi_k^e = \sum_{k'=1,K} \left(E_{kk'}^e\,\Psi_{k'}^e + \Gamma_{kk'}\,\Psi_{k'}^o\right), \tag{29}$$

$$\Delta_k^o\,\Psi_k^o = \Delta\Psi_k^o = \sum_{k'=1,K} \left(E_{kk'}^o\,\Psi_{k'}^o + \Gamma_{kk'}'\,\Psi_{k'}^e\right), \tag{30}$$

for $k = 1, K$. The TOMUHAWC code calculates the elements of the $\mathbf{E}^e$, $\mathbf{E}^o$, $\mathbf{\Gamma}$, and $\mathbf{\Gamma}'$ matrices, which only depend on the numerical solution of the linearized, marginally-stable, ideal-MHD equations in the outer region. On the other hand, the Δ_k^e and Δ_k^o values, which depend on the non-ideal layer solutions in the inner region, are not calculated by TOMUHAWC. The elements of the $\mathbf{E}^e$, $\mathbf{E}^o$, $\mathbf{\Gamma}$, and $\mathbf{\Gamma}'$ matrices are independent of the complex growth-rate, γ, of the instability, whereas the Δ_k^e and Δ_k^o values are generally functions of γ.

It is easily demonstrated that zero net toroidal electromagnetic torque is exerted on the plasma in the outer region as a consequence of tearing or twisting perturbations (see Sect. A 4).[9] On the other hand, the net torque exerted on the segment of the inner region centered on the kth rational surface is (see Sect. A 7)

$$\begin{aligned}\delta T_k &= 2\,n\,\pi^2\,\mathrm{Im}\left[\Delta\Psi_k^e\,\Psi_k^{e\,*} + \Delta\Psi_k^o\,\Psi_k^{o\,*}\right]\\ &= 2\,n\,\pi^2\left[\mathrm{Im}(\Delta_k^e)\,|\Psi_k^e|^{\,2} + \mathrm{Im}(\Delta_k^o)\,|\Psi_k^o|^{\,2}\right].\end{aligned} \tag{31}$$

Hence, making use of Eqs. (29) and (30), the total toroidal electromagnetic torque acting

on the plasma is

$$\begin{aligned} T_\phi &= \sum_{k=1,K} \delta T_k \\ &= n\,\pi^2\,\mathrm{Im}\left\{ \sum_{k,k'=1,K} \left[(E^e_{kk'} - E^{e\,*}_{k'k})\,\Psi^{e\,*}_k\,\Psi^e_{k'} + (E^o_{kk'} - E^{o\,*}_{k'k})\,\Psi^{o\,*}_k\,\Psi^o_{k'} \right.\right. \\ &\quad \left.\left. + 2\,(\Gamma_{kk'} - \Gamma'^{\,*}_{k'k})\,\Psi^{e\,*}_k\,\Psi^o_{k'} \right] \right\}. \end{aligned} \tag{32}$$

However, this total torque must be zero (because a plasma surrounded by a close fitting, axisymmetric, perfectly conducting wall cannot exert a net toroidal torque on itself). Moreover, this must be the case irrespective of the Ψ^e_k and Ψ^o_k values. It follows that (see Sect. A 8)

$$E^e_{kk'} = E^{e\,*}_{k'k}, \tag{33}$$

$$E^o_{kk'} = E^{o\,*}_{k'k}, \tag{34}$$

$$\Gamma'_{kk'} = \Gamma^*_{k'k} \tag{35}$$

for $k, k' = 1, K$. The extent to which these symmetries are respected is a sensitive test of the accuracy of the numerical solution in TOMUHAWC.

III. PLASMA EQUILIBRIUM

The up-down symmetric plasma equilibrium whose resistive stability is investigated in this paper is derived from the CHEASE code.[13] The plasma boundary is written parametrically as

$$R = R_c\left[1 + \bar{a}\,\cos(\omega + \bar{\delta}\,\sin\omega)\right], \tag{36}$$

$$Z = R_c\,\bar{a}\,\kappa\,\sin\omega \tag{37}$$

for $0 \leq \omega \leq 2\pi$. Here, $\bar{a}$ is the plasma minor radius, κ the elongation, and $\bar{\delta}$ the triangularity. The parameter R_c is automatically adjusted to ensure that the magnetic axis lies at $R = 1$. The chosen equilibrium profiles are

$$\frac{dP}{d\Psi} = P_0\left(\frac{\Psi}{\Psi_0}\right), \tag{38}$$

and

$$g(\Psi)\,\frac{dg}{d\Psi} = G_0\left(\frac{\Psi}{\Psi_0}\right)^{\nu}. \tag{39}$$

Here, $\Psi(r)$ is the poloidal magnetic flux [see Eq. (3)], and $\Psi_0 \equiv \Psi(0)$. The parameter G_0 is adjusted such that the central safety-factor, $q_0 \equiv q(0)$, takes a particular value. The parameter ν is adjusted such that the edge safety-factor, $q_a \equiv q(a)$, takes a particular value. Finally, the parameter P_0 is adjusted such that the normal beta,

$$\beta_N = \frac{\beta(\%)\,\bar{a}(\mathrm{m})\,B_0(\mathrm{T})}{I_p(\mathrm{MA})}, \tag{40}$$

takes a particular value. Here, the total toroidal current, I_p, and total plasma beta, β, are defined in Ref. 13.

In the example calculation considered in this paper, the parameters $\bar{a}$, κ, and δ are given the JET-like values 0.3. 1.8, and 0.25, respectively. Moreover, the chosen values of the central safety factor, the edge safety factor, and the normal beta are $q_0 = 1.05$, $q_a = 3.95$, and $\beta_N = 1.0$, respectively. The equilibrium safety-factor and pressure profiles are shown in Figs. 1 and 2, respectively, whereas the TOMUHAWC flux-coordinate system is illustrated in Fig. 3. The $q = 2$ and $q = 3$ surfaces lie at $r/a = 0.7507$ and $r/a = 0.9211$, respectively, where $a = 0.4039$.

IV. CALCULATION OF STABILITY MATRICES

Consider the stability of $n = 1$ resistive modes. The elements of the $\mathbf{E}^e$, $\mathbf{E}^o$, $\mathbf{\Gamma}$, and $\mathbf{\Gamma}'$ matrices, calculated by the TOMUHAWC code for the plasma equilibrium described in the

previous section, are as follows:

$$\mathbf{E}^e = \begin{pmatrix} +1.357\times 10^{+0}, & -6.058\times 10^{-1} \\ -6.058\times 10^{-1}, & -1.495\times 10^{+1} \end{pmatrix}, \tag{41}$$

$$\mathbf{E}^o = \begin{pmatrix} +1.046\times 10^{+2}, & +5.205\times 10^{+1} \\ +5.205\times 10^{+1}, & +9.950\times 10^{+1} \end{pmatrix}, \tag{42}$$

$$\mathbf{\Gamma} = \begin{pmatrix} +1.061\times 10^{+2}, & +1.854\times 10^{+1} \\ -3.107\times 10^{+1}, & +3.532\times 10^{+2} \end{pmatrix}, \tag{43}$$

$$\mathbf{\Gamma}' = \begin{pmatrix} +1.061\times 10^{+2}, & -3.107\times 10^{+1} \\ +1.854\times 10^{+1}, & +3.532\times 10^{+2} \end{pmatrix}. \tag{44}$$

Here, the first and second row/column of each matrix corresponds to the resonant poloidal mode numbers $m = 2$ and $m = 3$, respectively. The calculation is performed with $\delta/a = 10^{-7}$ and $\epsilon/a = 10^{-4}$, and includes all poloidal harmonics whose mode numbers lie in the range -13 to $+18$. Incidentally, in this example, the elements of the $\mathbf{E}^e$, $\mathbf{E}^o$, $\mathbf{\Gamma}$, and $\mathbf{\Gamma}'$ matrices are all real, because the equilibrium is up-down symmetric. Furthermore, the matrix elements satisfy the symmetry requirements (33)–(35) to a high degree of accuracy. (If this were not the case then the most likely cause would be a breakdown of the numerical method used in the code.) Finally, it has been verified that the above matrix elements are unaffected by any further decrease in the values of the numerical parameters δ and ϵ, or any further increase in the number of poloidal harmonics included in the calculation.

V. DETERMINATION OF LINEAR STABILITY

The complex growth-rates, γ, of $n = 1$ resistive instabilities in our example equilibrium are determined by solving the following equation:

$$\begin{vmatrix} E^e_{11} - \Delta^e_1(\gamma), & E^e_{12}, & \Gamma_{11}, & \Gamma_{12} \\ E^e_{12}, & E^e_{22} - \Delta^e_2(\gamma), & \Gamma_{21}, & \Gamma_{22} \\ \Gamma_{11}, & \Gamma_{21}, & E^o_{11} - \Delta^o_1(\gamma), & E^o_{12} \\ \Gamma_{12}, & \Gamma_{22}, & E^o_{21}, & E^o_{22} - \Delta^o_2(\gamma) \end{vmatrix} = 0. \tag{45}$$

Here, the complex quantities $\Delta^e_1(\gamma)$, $\Delta^o_1(\gamma)$, $\Delta^e_2(\gamma)$, and $\Delta^o_2(\gamma)$ are, respectively, the layer stability parameter for tearing parity modes at the $q = 2$ surface, the corresponding param-

eter for twisting parity modes, the layer stability parameter for tearing parity modes at the $q = 3$ surface, and the corresponding parameter for twisting parity modes. As described in Appendix B, these quantities are determined by solving the equations of linearized resistive-MHD in thin layers centered on the $q = 2$ and $q = 3$ surfaces. (In fact, the layer equations are solved numerically using the finite difference method described in Ref. 14.) In general, we can write

$$\Delta_k^{e,o} = S_k^{(2/3)\sqrt{D_{I\,k}}}\,\tilde{\Delta}_k^{e,o}(\tilde{Q}_k, E_k + F_k, H_k, K_k\,E_k - G_k, K_k\,F_k + H_k, K_k\,H_k, f_{A\,k}, f_{S\,k}), \quad (46)$$

where

$$\gamma = \mathrm{i}\,n\,\Omega_k + \tilde{Q}_k\,S_k^{-1/3}\,\omega_{A\,k}. \quad (47)$$

Here, S_k is the magnetic Lundquist number, Ω_k the plasma toroidal angular velocity, and $\omega_{A\,k}$ the shear-Alfvén frequency [see Eq. (B47)], all evaluated at the kth rational surface. Moreover, E_k, F_k, G_k, H_k, and K_k are standard Glasser-Greene-Johnson layer parameters [2] [see Eqs. (B25)–(B29)], evaluated at the same surface. Note that

$$D_{I\,k} = \frac{1}{4} - E_k - F_k - H_k. \quad (48)$$

Finally, the parameters $f_{S\,k}$ and $f_{A\,k}$ are defined in Eqs. (B52) and (B53), respectively. The values of the various layer parameters for the plasma equilibrium under consideration are listed in Table I.

The dispersion relation (45) can be written

$$\begin{vmatrix} E_{11}^e - S_1^{(2/3)\sqrt{D_{I\,1}}}\,\tilde{\Delta}_1^e, & E_{12}^e, & \Gamma_{11}, & \Gamma_{12} \\ E_{12}^e, & E_{22}^e - S_2^{(2/3)\sqrt{D_{I\,2}}}\,\tilde{\Delta}_2^e, & \Gamma_{21}, & \Gamma_{22} \\ \Gamma_{11}, & \Gamma_{21}, & E_{11}^o - S_1^{(2/3)\sqrt{D_{I\,1}}}\,\tilde{\Delta}_1^o, & E_{12}^o \\ \Gamma_{12}, & \Gamma_{22}, & E_{21}^o, & E_{22}^o - S_2^{(2/3)\sqrt{D_{I\,2}}}\,\tilde{\Delta}_2^o \end{vmatrix} = 0. \quad (49)$$

Here, the normalized layer stability parameters, $\tilde{\Delta}_{1,2}^{e,o}$, as well as the elements of the $\mathbf{E}^{e,o}$ and $\mathbf{\Gamma}$ matrices, are independent of the Lundquist numbers, S_1 and S_2, at the two rational surfaces. Now, it is apparent that, in the limit of very high Lundquist numbers, $S_1, S_2 \to \infty$, the four roots of the above dispersion relation correspond to $\tilde{\Delta}_1^e = 0$, $\tilde{\Delta}_1^o = 0$, $\tilde{\Delta}_2^e = 0$, and $\tilde{\Delta}_2^o = 0$. Moreover, these roots can be identified as a tearing parity mode that only reconnects magnetic flux at the $q = 2$ surface, a twisting parity mode that only reconnects flux at the

same surface, a tearing parity mode that only reconnects magnetic flux at the $q = 3$ surface, and a twisting parity mode that only reconnects flux at the same surface, respectively. The normalized growth-rates of these four modes are

$$\tilde{Q}_1^e = -8.458 \times 10^{-2} \pm 1.465 \times 10^{-1}\,\mathrm{i}, \tag{50}$$

$$\tilde{Q}_1^o = -1.488 \times 10^{-1} \pm 2.578 \times 10^{-1}\,\mathrm{i}, \tag{51}$$

$$\tilde{Q}_2^e = -1.678 \times 10^{-2} \pm 2.906 \times 10^{-2}\,\mathrm{i}, \tag{52}$$

$$\tilde{Q}_2^o = -3.024 \times 10^{-2} \pm 5.238 \times 10^{-2}\,\mathrm{i}, \tag{53}$$

respectively. The corresponding unnormalized growth-rates are obtained from Eq. (47). Thus, it is clear that, in the very high Lundquist number limit, the resistive stability of the plasma is determined by layer physics at the various rational surfaces within the plasma, and is completely independent of the outer solution. It follows from Eqs. (50)–(53) that the particular plasma equilibrium under investigation is stable to $n = 1$ resistive modes in the very high Lundquist number limit. This is a general result, and is a consequence of the stabilizing influence of the characteristic favorable average magnetic field-line curvature of a tokamak plasma (for $q \geq 1$ and $dp/dr > 0$), which becomes a dominant effect at high Lundquist number.[2]

In a realistic tokamak plasma, the Lundquist numbers at the two rational surfaces are large, but finite, so that $0 \leq 1/S_1, 1/S_2 \ll 1$. In this case, the dispersion relation (49) can have non-trivial roots [i.e., roots significantly different from (50)–(53)] provided that $0 \leq |\tilde{\Delta}_1^e| \ll 1$, or $0 \leq |\tilde{\Delta}_1^o| \ll 1$, or $0 \leq |\tilde{\Delta}_2^e| \ll 1$, or $0 \leq |\tilde{\Delta}_2^o| \ll 1$. Figures 4 and 5 illustrate the behavior of $|\tilde{\Delta}_1^e|$ and $|\tilde{\Delta}_1^o|$ in the vicinity of the trivial roots (50) and (51). [The behavior of $|\tilde{\Delta}_2^e|$ and $|\tilde{\Delta}_2^o|$ in the vicinity of the roots (52) and (53) is analogous.] It can be seen that $|\tilde{\Delta}_1^o|$ is only small compared to unity when $\tilde{Q}_1$ lies extremely close to the root (52). On the other hand, $|\tilde{\Delta}_1^e|$ is generally small compared to unity as long as $|\tilde{Q}_1|$ is small compared to unity. Likewise, $|\tilde{\Delta}_2^o|$ is only small when $\tilde{Q}_2$ lies extremely close to the root (52), whereas $|\tilde{\Delta}_2^e|$ is small as long as $|\tilde{Q}_2|$ is small. Consequently, at large but finite Lundquist numbers, the roots of the dispersion relation (49) are given approximately by

$$\left| \begin{array}{ll} E_{11}^e - S_1^{(2/3)\sqrt{D_{I\,1}}}\,\tilde{\Delta}_1^e, & E_{12}^e \\ E_{12}^e, & E_{22}^e - S_2^{(2/3)\sqrt{D_{I\,2}}}\,\tilde{\Delta}_2^e \end{array} \right| \simeq 0, \tag{54}$$

and

$$\tilde{\Delta}_1^o \simeq 0, \tag{55}$$

$$\tilde{\Delta}_2^o \simeq 0. \tag{56}$$

However, it is apparent from Eq. (47) that if

$$n\,|\Omega_1 - \Omega_2| \gg S_1^{-1/3}\,\omega_{A\,1},\, S_2^{-1/3}\,\omega_{A\,2}, \tag{57}$$

as is likely to be the case in a tokamak plasma possessing moderate toroidal velocity shear, then $|\tilde{\Delta}_2^e| \gg 1$ whenever $|\tilde{\Delta}_1^e| \ll 1$, and vice versa (because $|\tilde{Q}_1| \gg 1$ whenever $|\tilde{Q}_2| \ll 1$, and vice versa).[9,10,15] In this situation, the roots of the dispersion relation (49) are given approximately by

$$S_1^{(2/3)\sqrt{D_{I\,1}}}\,\tilde{\Delta}_1^e \equiv \Delta_1^e \simeq E_{11}^e, \tag{58}$$

$$S_2^{(2/3)\sqrt{D_{I\,2}}}\,\tilde{\Delta}_2^e \equiv \Delta_2^e \simeq E_{22}^e, \tag{59}$$

$$\Delta_1^o \simeq 0, \tag{60}$$

$$\Delta_2^o \simeq 0. \tag{61}$$

These roots correspond, respectively, to a tearing parity mode that only reconnects magnetic flux at the $q = 2$ surface, a tearing parity mode that only reconnects magnetic flux at the $q = 3$ surface, a twisting parity mode that only reconnects magnetic flux at the $q = 2$ surface, and a twisting parity mode that only reconnects magnetic flux at the $q = 3$ surface.

Figure 6 shows the normalized $n = 1$ growth-rate of the tearing parity mode that reconnects magnetic flux at the $q = 2$ surface, $\tilde{Q}_1$, calculated with the resonant layer parameters listed in Table I as a function of the normalized tearing parity layer stability parameter, $\tilde{\Delta}_1^e$ (which is assumed to be real). It can be seen that the mode becomes unstable when $\tilde{\Delta}_1^e$ exceeds the critical value $\tilde{\Delta}_{1\,\rm crit}^e = 9.643\times10^{-2}$. Similarly, the tearing parity mode that reconnects magnetic flux at the $q = 3$ surface becomes unstable when $\tilde{\Delta}_2^e > \tilde{\Delta}_{2\,\rm crit}^e = 4.228\times10^{-2}$. We conclude that, for the equilibrium in question, the $n = 1$ twisting parity modes that only reconnect magnetic flux at the $q = 2$ and $q = 3$ surfaces are both linearly stable [because Eqs. (60) and (61) are only satisfied by modes whose growth-rates have negative real parts]. Morover, according to Equation (59), the $n = 1$ tearing parity mode that only reconnects flux at the $q = 3$ surface is also linearly stable (because $E_{22}^e < 0$, so it is impossible for $\tilde{\Delta}_2^e$

to exceed $\tilde{\Delta}^e_{2\,\rm crit}$). On the other hand, according to Equation (58), the $n = 1$ tearing parity mode that only reconnects flux at the $q = 2$ surface becomes linearly unstable when the Lundquist number at the surface in question surface falls below the critical value

$$S_{1\,\rm crit} = \left(\frac{E^e_{11}}{\tilde{\Delta}^e_{1\,\rm crit}}\right)^{(3/2)/\sqrt{D_{I\,1}}} = \left(\frac{1.357\times 10^{+0}}{9.643\times 10^{-2}}\right)^{1.5/\sqrt{0.2795}} = 1.81\times 10^3. \tag{62}$$

The eigenfunction of this potentially unstable mode is shown in Fig. 7.

VI. SUMMARY

This paper describes the recently developed TOMUHAWC code, which is designed to investigate the global resistive stability of high temperature tokamak plasmas with realistic equilibria. The code solves (by means of adaptive-step integration) the linearized, Fourier transformed, marginally-stable (i.e., zero inertia), ideal-MHD equations everywhere in the plasma except in the immediate vicinity of the various rational flux-surfaces, where the equations are singular. The equations are matched asymptotically across the rational surfaces to determine the elements of the so-called stability matrix. This matrix is calculated for both tearing and twisting parity modes.

The analysis underlying the TOMUHAWC code (including the specification of the metric data required by the code, and the definition of the stability matrix) is summarized in Sect. II, and described in detail in Appendix A.

An illustration of the use of the code to determine the linear global resistive stability of a specified fixed boundary tokamak plasma equilibrium is given in Sects III–V. To be more exact, in Sect. IV, the $n = 1$ stability matrix is calculated for an up-down symmetric JET-like equilibrium containing two coupled rational surfaces (namely, the $q = 2$ and $q = 3$ surfaces). The equilibrium itself is described in Sect. III. In Sect. V, the stability matrix data is combined with a Glasser-Green-Johnson linear layer model (described in Appendix B) to determine the linear stability of $n = 1$ resistive modes for the equilibrium in question. It is demonstrated that the large Lundquist numbers, and moderate levels of toroidal velocity shear, prevalent in modern tokamak plasmas give rise to a decoupling of tearing and twisting parity modes that only reconnect magnetic flux at a single rational surface in the plasma, and whose resistive stability can, therefore, be determined independently. The twisting parity modes that only reconnect flux at the $q = 2$ and $q = 3$ surfaces are found to be robustly

stable. The tearing parity mode that only reconnects flux at the $q = 3$ surface is also found to be robustly stable. Finally, the tearing parity mode that only reconnects flux at the $q = 2$ surface is found to be stable as long as the Lundquist number at the surface remains above a critical value that is of order 10^3.

ACKNOWLEDGEMENTS

This research was funded by the U.S. Department of Energy under contract DE-FG02-04ER-54742.

---

[1] H.P. Furth, J. Killeen, and M.N. Rosenbluth, Phys. Fluids **6**, 459 (1963).

[2] A.H. Glasser, J.M. Greene, and J.L. Johnson, Phys. Fluids **18**, 875 (1975).

[3] J.W. Connor, R.J. Hastie, and J.B. Taylor, Phys. Fluids B **3**, 1539 (1991).

[4] A. Pletzer, and R.L. Dewar, J. Plasma Phys. **45**, 427 (1991).

[5] R.L. Dewar, and M. Persson, Phys. Fluids B **5**, 4273 (1993).

[6] A. Pletzer, A. Bondeson, and R.L. Dewar, Jou. Comp. Physics **115**, 530 (1994).

[7] R. Fitzpatrick, Phys. Plasmas **1**, 3308 (1994).

[8] J.W. Connor, S.C. Cowley, R.J. Hastie, T.C. Hender, A. Hood, and T.J. Martin, Phys. Fluids **31**, 577 (1988).

[9] R. Fitzpatrick, R.J. Hastie, T.J. Martin, and C.M. Roach, Nucl. Fusion **33**, 1533 (1993).

[10] C.J. Ham, J.W. Connor, S.C. Cowley, C.G. Gimblett, R.J. Hastie, T.C. Hender, and T.J. Martin, Plasma Phys. Control. Fusion **54**, 025009 (2012).

[11] J.R. Dormand, and P.J. Prince, Jou. Comp. Applied Math. **6**. 19 (1980).

[12] C. Mercier, Nucl. Fusion **1**, 47 (1960).

[13] H. Lütjens, A. Bondeson, and O. Sauter, Comp. Phys. Comm. **97**, 219 (1996).

[14] A.H. Glasser, S.C. Jardin, and G. Tesauro, Phys. Fluids **27**, 1225 (1984).

[15] S.C. Cowley, and R.J. Hastie, Phys. Fluids **31**, 426 (1998).

Appendix A: Solution of Linearized Marginally-Stable Ideal-MHD Equations

1. Normalization and Coordinates

All lengths are normalized to the major radius of the plasma magnetic axis, R_0, all magnetic field-strengths to the vacuum toroidal field-strength at the magnetic axis, B_0, and all plasma pressures to B_0^2/μ_0.

Let R, ϕ, Z be right-handed cylindrical coordinates whose symmetry axis corresponds to the toroidal symmetry axis of the plasma. The Jacobian for these coordinates is

$$(\nabla R \times \nabla\phi \cdot \nabla Z)^{-1} = R. \tag{A1}$$

Let r, θ, ϕ be right-handed flux coordinates whose Jacobian is [8,9]

$$\mathcal{J}(r,\theta) \equiv (\nabla r \times \nabla\theta \cdot \nabla\phi)^{-1} = r\,R^2. \tag{A2}$$

Here, r is a flux-surface label with dimensions of length. Furthermore, θ is a "straight" poloidal angle. Let $r = 0$ correspond to the magnetic axis, and $\theta = 0$ to the inboard midplane.

2. Plasma Equilibrium

Consider an axisymmetric tokamak plasma equilibrium. The magnetic field is written [8,9]

$$\mathbf{B}(r,\theta) = f(r)\,\nabla\phi \times \nabla r + g(r)\,\nabla\phi = f\,\nabla(\phi - q\,\theta) \times \nabla r, \tag{A3}$$

where

$$q(r) = \frac{r\,g}{f} \tag{A4}$$

is the safety-factor profile. It is assumed that $g = 1$ at the plasma boundary.

Equilibrium force balance yields the Grad-Shafranov equation,[8,9]

$$\frac{1}{r}\,\frac{\partial}{\partial r}\left(r\,f\,|\nabla r|^2\right) + \frac{1}{r}\,\frac{\partial}{\partial\theta}\left(r\,f\,\nabla r\cdot\nabla\theta\right) + \frac{g\,g'}{f} + \left(\frac{R}{R_0}\right)^2\frac{P'}{f} = 0, \tag{A5}$$

where $P(r)$ is the plasma pressure profile, and $' \equiv d/dr$.

3. Governing Equations

Consider a small perturbation to the previously described plasma equilibrium. The system is conveniently divided into an "outer region" and an "inner region".[1] The outer region comprises all of the plasma except a number of radially thin layers centered on the various rational surfaces. The inner region consists of the aforementioned layers. The perturbation in the outer region is governed by linearized, marginally-stable, ideal-MHD, whereas that in the inner region is governed by either linear or nonlinear resistive-MHD.[1] The overall solution is constructed by asymptotically matching the ideal-MHD solution in the outer region to the resistive-MHD solutions in the various segments of the inner region.

The linearized, marginally-stable, ideal-MHD equations that govern the perturbation in the outer region are[1]

$$\delta\mathbf{B} = \nabla \times (\boldsymbol{\xi} \times \mathbf{B}), \tag{A6}$$

$$\nabla\delta P = \delta\mathbf{J} \times \mathbf{B} + \mathbf{J} \times \delta\mathbf{B}, \tag{A7}$$

$$\delta\mathbf{J} = \nabla \times \delta\mathbf{B}, \tag{A8}$$

$$\delta P = -\boldsymbol{\xi} \cdot \nabla P. \tag{A9}$$

Here, $\mathbf{J} = \nabla \times \mathbf{B}$ is the equilibrium current density. Moreover, $\boldsymbol{\xi}$, $\delta\mathbf{B}$, $\delta\mathbf{J}$, and δP are the plasma displacement, perturbed magnetic field, perturbed current density, and perturbed pressure, respectively.

4. Fourier Transformed Equations

Let

$$f\,\boldsymbol{\xi} \cdot \nabla r = y(r,\theta)\,\exp(-\mathrm{i}\,n\,\phi), \tag{A10}$$

$$R^2\,\delta\mathbf{B} \cdot \nabla\phi = z(r,\theta)\,\exp(-\mathrm{i}\,n\,\phi), \tag{A11}$$

where $n > 0$ is the toroidal mode number of the perturbation. After considerable algebra, Eqs. (A6)–(A9) reduce to [8,9]

$$r\,\frac{\partial}{\partial r}\left[\left(\frac{\partial}{\partial\theta}-\mathrm{i}\,n\,q\right)y\right]=\frac{\partial}{\partial\theta}\left(Q\,\frac{\partial z}{\partial\theta}\right)+S\,z-\frac{\partial}{\partial\theta}\left[T\left(\frac{\partial}{\partial\theta}-\mathrm{i}\,n\,q\right)y+U\,y\right], \tag{A12}$$

$$\left(\frac{\partial}{\partial\theta}-\mathrm{i}\,n\,q\right)r\,\frac{\partial z}{\partial r}=-\left(\frac{\partial}{\partial\theta}-\mathrm{i}\,n\,q\right)T^{*}\,\frac{\partial z}{\partial\theta}+U\,\frac{\partial z}{\partial\theta}+X\,y$$
$$-\left(\frac{\partial}{\partial\theta}-\mathrm{i}\,n\,q\right)V\left(\frac{\partial}{\partial\theta}-\mathrm{i}\,n\,q\right)y+W\left(\frac{\partial}{\partial\theta}-\mathrm{i}\,n\,q\right)y, \tag{A13}$$

where

$$Q(r,\theta)=\frac{1}{\mathrm{i}\,n\,|\nabla r|^{\,2}}, \tag{A14}$$

$$S(r,\theta)=\mathrm{i}\,n\,\alpha_{\epsilon}, \tag{A15}$$

$$T(r,\theta)=\frac{r\,\nabla r\cdot\nabla\theta}{|\nabla r|^{\,2}}-\frac{\alpha_g}{\mathrm{i}\,n\,|\nabla r|^{\,2}}, \tag{A16}$$

$$U(r,\theta)=\frac{\alpha_p}{|\nabla r|^{\,2}}\left(\frac{R}{R_0}\right)^{2}, \tag{A17}$$

$$V(r,\theta)=\frac{1}{|\nabla r|^{\,2}}\left[\mathrm{i}\,n\left(\frac{R_0}{R}\right)^{2}+\frac{\alpha_g^{\,2}}{\mathrm{i}\,n}\right], \tag{A18}$$

$$W(r,\theta)=\frac{2\,\alpha_g\,\alpha_p}{|\nabla r|^{\,2}}\left(\frac{R}{R_0}\right)^{2}-r\,\frac{d\alpha_g}{dr}, \tag{A19}$$

$$X(r,\theta)=\mathrm{i}\,n\,\alpha_p\left[\frac{\partial}{\partial\theta}\left\{T^{*}\left(\frac{R}{R_0}\right)^{2}\right\}+r\,\frac{\partial}{\partial r}\left(\frac{R}{R_0}\right)^{2}-\alpha_f\left(\frac{R}{R_0}\right)^{2}-U\left(\frac{R}{R_0}\right)^{2}\right], \tag{A20}$$

and

$$\alpha_{\epsilon}(r)=r^{2}, \tag{A21}$$

$$\alpha_g(r)=\frac{1}{f}\,\frac{dg}{dr}, \tag{A22}$$

$$\alpha_p(r)=\frac{r}{f^{\,2}}\,\frac{dP}{dr}, \tag{A23}$$

$$\alpha_f(r)=\frac{r^{2}}{f}\,\frac{d}{dr}\left(\frac{f}{r}\right). \tag{A24}$$

Let

$$y(r,\theta)=\sum_{j=1,J}y_j(r)\,\exp(\,\mathrm{i}\,m_j\,\theta), \tag{A25}$$

$$z(r,\theta)=\sum_{j=1,J}z_j(r)\,\exp(\,\mathrm{i}\,m_j\,\theta), \tag{A26}$$

where the m_j, for $j = 1, J$, are the various coupled poloidal harmonics included in the calculation. Equations (A12) and (A13) reduce to

$$r\,\frac{d}{dr}\left[(m_j - n\,q)\,y_j\right] = \sum_{j'=1,J}\left(B_{jj'}\,z_{j'} + C_{jj'}\,y_{j'}\right), \tag{A27}$$

$$(m_j - n\,q)\,r\,\frac{dz_j}{dr} = \sum_{j'=1,J}\left(D_{jj'}\,z_{j'} + E_{jj'}\,y_{j'}\right), \tag{A28}$$

for $j = 1, J$, where

$$B_{jj'}(r) = \frac{1}{2\pi\,\mathrm{i}}\oint \mathrm{e}^{-\mathrm{i}\,m_j\,\theta}\left(\frac{\partial}{\partial\theta}\,Q\,\frac{\partial}{\partial\theta} + S\right)\mathrm{e}^{\,\mathrm{i}\,m_{j'}\,\theta}\,d\theta, \tag{A29}$$

$$C_{jj'}(r) = \frac{1}{2\pi\,\mathrm{i}}\oint \mathrm{e}^{-\mathrm{i}\,m_j\,\theta}\left[-\frac{\partial}{\partial\theta}\,T\left(\frac{\partial}{\partial\theta} - \mathrm{i}\,n\,q\right) - \frac{\partial U}{\partial\theta}\right]\mathrm{e}^{\,\mathrm{i}\,m_{j'}\,\theta}\,d\theta, \tag{A30}$$

$$D_{jj'}(r) = \frac{1}{2\pi\,\mathrm{i}}\oint \mathrm{e}^{-\mathrm{i}\,m_j\,\theta}\left[-\left(\frac{\partial}{\partial\theta} - \mathrm{i}\,n\,q\right)T^*\,\frac{\partial}{\partial\theta} + U\,\frac{\partial}{\partial\theta}\right]\mathrm{e}^{\,\mathrm{i}\,m_{j'}\,\theta}\,d\theta, \tag{A31}$$

$$\begin{aligned} E_{jj'}(r) = \frac{1}{2\pi\,\mathrm{i}}\oint \mathrm{e}^{-\mathrm{i}\,m_j\,\theta}\Bigg[&-\left(\frac{\partial}{\partial\theta} - \mathrm{i}\,n\,q\right)V\left(\frac{\partial}{\partial\theta} - \mathrm{i}\,n\,q\right) \\ &+ W\left(\frac{\partial}{\partial\theta} - \mathrm{i}\,n\,q\right) + X\Bigg]\mathrm{e}^{\,\mathrm{i}\,m_{j'}\,\theta}\,d\theta. \end{aligned} \tag{A32}$$

Hence, it follows from Eqs. (A14)–(A20) that

$$n\,B_{jj'} = m_j\,m_{j'}\,c_{jj'} + n^2\,\alpha_\epsilon\,\delta_{jj'}, \tag{A33}$$

$$C_{jj'} = m_j\,(m_{j'} - n\,q)\left(-f_{jj'} + n^{-1}\,\alpha_g\,c_{jj'}\right) - m_j\,\alpha_p\,d_{jj'}, \tag{A34}$$

$$D_{jj'} = -\,(m_j - n\,q)\,m_{j'}\left(f_{jj'} + n^{-1}\,\alpha_g\,c_{jj'}\right) + m_{j'}\,\alpha_p\,d_{jj'}, \tag{A35}$$

$$\begin{aligned} n^{-1}\,E_{jj'} = &\,(m_j - n\,q)\,(m_{j'} - n\,q)\left(b_{jj'} - n^{-2}\,\alpha_g^2\,c_{jj'}\right) - (m_{j'} - n\,q)\,n^{-1}\,r\,\frac{d\alpha_g}{dr}\,\delta_{jj'} \\ &+ \alpha_p\left[(m_j - m_{j'})\,g_{jj'} + n^{-1}\,\alpha_g\,(m_j + m_{j'} - 2\,n\,q)\,d_{jj'} + r\,\frac{da_{jj'}}{dr}\right. \\ &\left.-\alpha_f\,a_{jj'} - \alpha_p\,e_{jj'}\right], \end{aligned} \tag{A36}$$

where

$$a_{jj'}(r) = \oint R^2 \exp\left[-\mathrm{i}\,(m_j - m_{j'})\,\theta\right] \frac{d\theta}{2\pi}, \tag{A37}$$

$$b_{jj'}(r) = \oint |\nabla r|^{-2}\, R^{-2} \exp\left[-\mathrm{i}\,(m_j - m_{j'})\,\theta\right] \frac{d\theta}{2\pi}, \tag{A38}$$

$$c_{jj'}(r) = \oint |\nabla r|^{-2} \exp\left[-\mathrm{i}\,(m - m')\,\theta\right] \frac{d\theta}{2\pi}, \tag{A39}$$

$$d_{jj'}(r) = \oint |\nabla r|^{-2}\, R^2 \exp\left[-\mathrm{i}\,(m_j - m_{j'})\,\theta\right] \frac{d\theta}{2\pi}, \tag{A40}$$

$$e_{jj'}(r) = \oint |\nabla r|^{-2}\, R^4 \exp\left[-\mathrm{i}\,(m_j - m_{j'})\,\theta\right] \frac{d\theta}{2\pi}, \tag{A41}$$

$$f_{jj'}(r) = \oint \frac{\mathrm{i}\, r\, \nabla r\cdot\nabla\theta}{|\nabla r|^2} \exp\left[-\mathrm{i}\,(m_j - m_{j'})\,\theta\right] \frac{d\theta}{2\pi}, \tag{A42}$$

$$g_{jj'}(r) = \oint \frac{\mathrm{i}\, r\, \nabla r\cdot\nabla\theta}{|\nabla r|^2}\, R^2 \exp\left[-\mathrm{i}\,(m_j - m_{j'})\,\theta\right] \frac{d\theta}{2\pi}. \tag{A43}$$

Let

$$y_j = \frac{\psi_j(r)}{m_j - n\,q}, \tag{A44}$$

$$z_j = n\,\frac{Z_j(r)}{m_j - n\,q} - \frac{C_{jj}}{B_{jj}}\,\frac{\psi_j(r)}{m_j - n\,q}. \tag{A45}$$

It follows that

$$\delta\mathbf{B}\cdot\nabla r = \mathrm{i}\, R^{-2} \sum_{j=1,J} \frac{\psi_j}{r}\, \exp[\,\mathrm{i}\,(m_j\,\theta - n\,\phi)]. \tag{A46}$$

Furthermore, Eqs. (A27) and (A28) transform to

$$r\,\frac{d\psi_j}{dr} = \sum_{j'=1,J} \frac{L_{jj'}\,Z_{j'} + M_{jj'}\,\psi_{j'}}{m_{j'} - n\,q}, \tag{A47}$$

$$(m_j - n\,q)\,r\,\frac{d}{dr}\left(\frac{Z_j}{m_j - n\,q}\right) = \sum_{j'=1,J} \frac{N_{jj'}\,Z_{j'} + P_{jj'}\,\psi_{j'}}{m_{j'} - n\,q}, \tag{A48}$$

for $j = 1, J$, where

$$L_{jj'}(r) = n\,B_{jj'}, \tag{A49}$$

$$M_{jj'}(r) = C_{jj'} + \lambda_{j'}\,L_{jj'}, \tag{A50}$$

$$N_{jj'}(r) = D_{jj'} - \lambda_j\,L_{jj'}, \tag{A51}$$

$$\begin{aligned} P_{jj'}(r) = {} & n^{-1}\,E_{jj'} - \lambda_j\,M_{jj'} + \lambda_{j'}\,N_{jj'} + \lambda_j\,\lambda_{j'}\,L_{jj'} \\ & - \lambda_j\,n\,q\,s\,\delta_{jj'} - (m_j - n\,q)\,r\,\frac{d\lambda_j}{dr}\,\delta_{jj'}, \end{aligned} \tag{A52}$$

with

$$s(r) = \frac{r\,q'}{q}, \tag{A53}$$

and

$$\lambda_j(r) = -\frac{C_{jj}}{n\,B_{jj}} = -\left[\frac{m_j\,(m_j - n\,q)\,n^{-1}\,\alpha_g\,c_{jj} - m\,\alpha_p\,d_{jj}}{m_j^2\,c_{jj} + n^2\,\alpha_\epsilon}\right]. \tag{A54}$$

Now, for a general plasma equilibrium, it is easily demonstrated that $a_{j'j} = a^*_{jj'}$, $b_{j'j} = b^*_{jj'}$, $c_{j'j} = c^*_{jj'}$, $d_{j'j} = d^*_{jj'}$, $e_{j'j} = e^*_{jj'}$, $f_{j'j} = -f^*_{jj'}$, $g_{j'j} = -g^*_{jj'}$, for all j, j', so that $B_{j'j} = B^*_{jj'}$, $C_{j'j} = -D^*_{jj'}$, $D_{j'j} = -C^*_{jj'}$, $E_{j'j} = E^*_{jj'}$, and

$$L_{j'j} = L^*_{jj'}, \tag{A55}$$

$$M_{j'j} = -N^*_{jj'}, \tag{A56}$$

$$N_{j'j} = -M^*_{jj'}, \tag{A57}$$

$$P_{j'j} = P^*_{jj'}. \tag{A58}$$

It follows from Eqs. (A47) and (A48) that

$$r\,\frac{d}{dr}\left(\sum_{j=1,J}\frac{Z_j^*\,\psi_j - \psi_j^*\,Z_j}{m_j - n\,q}\right) = 0. \tag{A59}$$

The net toroidal electromagnetic torque acting on the region lying within that equilibrium magnetic flux-surface whose label is r takes the form[9]

$$T_\phi(r) = \int_0^r \oint\oint R^2\,\nabla\phi\cdot(\delta\mathbf{J}\times\delta\mathbf{B})\,\mathcal{J}\,dr\,d\theta\,d\phi, \tag{A60}$$

which can be shown to reduce to

$$T_\phi(r) = n\,\pi^2\,\mathrm{i}\sum_{j=1,J}\frac{Z_j^*\,\psi_j - \psi_j^*\,Z_j}{m_j - n\,q}. \tag{A61}$$

Hence, we deduce that

$$\frac{dT_\phi}{dr} = 0 \tag{A62}$$

in the outer region.

5. Behavior in Vicinity of Rational Surface

Let there be K rational surfaces in the plasma. Suppose that the kth surface has the flux-surface label r_k, and the resonant poloidal mode number m_k, where $q(r_k) = m_k/n$, for $k = 1, K$.

Consider the solution of the outer equations, (A47) and (A48), in the vicinity of the kth surface. Let $x = r - r_k$. The most general small-$|x|$ solution of the outer equations can be shown to take the form [9]

$$\psi_j(x) = A^{\pm}_{L\,k}\,|x|^{\nu_{L\,k}}\,(1 + \lambda_{L\,k}\,x + \cdots) + A^{\pm}_{S\,k}\,\mathrm{sgn}(x)\,|x|^{\nu_{S\,k}}\,(1 + \cdots) + A_{C\,k}\,x\,(1 + \cdots), \tag{A63}$$

$$Z_j(x) = A^{\pm}_{L\,k}\,|x|^{\nu_{L\,k}}(b_{L\,k} + \gamma_{L\,k}\,x + \cdots) + A^{\pm}_{S\,k}\,\mathrm{sgn}(x)\,|x|^{\nu_{S\,k}}\,(b_{S\,k} + \cdots) + B_{C\,k}\,x\,(1 + \cdots) \tag{A64}$$

if $m_j = m_k$, and

$$\psi_j(x) = A^{\pm}_{L\,k}\,|x|^{\nu_{L\,k}}\,(a_{kj} + \cdots) + \bar{\psi}_{kj}\,(1 + \cdots), \tag{A65}$$

$$Z_j(x) = A^{\pm}_{L\,k}\,|x|^{\nu_{L\,k}}\,(b_{kj} + \cdots) + \bar{Z}_{kj}\,(1 + \cdots) \tag{A66}$$

if $m_j \neq m_k$. Moreover, the superscripts $^+$ and $^-$ correspond to $x > 0$ and $x < 0$, respectively. Here,

$$\nu_{L\,k} = \frac{1}{2} - \sqrt{D_{I\,k}}, \tag{A67}$$

$$\nu_{S\,k} = \frac{1}{2} + \sqrt{D_{I\,k}}, \tag{A68}$$

$$D_{I\,k} = \frac{1}{4} + L_{0\,k}\,P_{0\,k}, \tag{A69}$$

$$L_{0\,k} = -\left(\frac{L_{kk}}{m_k\,s}\right)_{r_k}, \tag{A70}$$

$$P_{0\,k} = -\left(\frac{P_{kk}}{m_k\,s}\right)_{r_k}. \tag{A71}$$

Furthermore,

$$b_{L\,k} = \frac{\nu_{L\,k}}{L_{0\,k}}, \tag{A72}$$

$$b_{S\,k} = \frac{\nu_{S\,k}}{L_{0\,k}}, \tag{A73}$$

$$A_{C\,k} = -\frac{1}{r_k\,P_{0\,k}} \sum_{j=1,J}^{m_j \neq m_k} \frac{1}{m_j - m_k} \left(N_{k\,j}\,\bar{Z}_{kj} + P_{kj}\,\bar{\psi}_{kj}\right)_{r_k}, \tag{A74}$$

$$B_{C\,k} = -\frac{1}{r_k\,L_{0\,k}} \sum_{j=1,J}^{m_j \neq m_k} \frac{1}{m_j - m_k} \left(L_{kj}\,\bar{Z}_{kj} + M_{kj}\,\bar{\psi}_{kj}\right)_{r_k} + \frac{A_{C\,k}}{L_{0\,k}}, \tag{A75}$$

$$\begin{aligned}\lambda_{L\,k} = {} & \frac{1}{2\,r_k}\left[\frac{P_{1\,k}\,L_{0\,k}}{\nu_{L\,k}} + T_{1\,k} + \nu_{L\,k}\left(\frac{L_{1\,k}}{L_{0\,k}} - 2\right)\right]_{r_k} \\ & - \frac{1}{(m_k\,s)_{r_k}}\,\frac{1}{r_k\,\nu_{L\,k}} \sum_{j=1,J}^{m_j \neq m_k} \frac{1}{m_j - m_k} \left(P_{kj}\,L_{kj} - M_{kj}\,N_{kj}\right)_{r_k},\end{aligned} \tag{A76}$$

$$\begin{aligned}\gamma_{L\,k} = {} & \frac{1}{2\,r_k}\left[(1+\nu_{L\,k})\left(\frac{P_{1\,k}}{\nu_{L\,k}} + \frac{T_{1\,k}}{L_{0\,k}} - \frac{\nu_{L\,k}}{L_{0\,k}}\right) + P_{0\,k}\left(\frac{L_{1\,k}}{L_{0\,k}} - 1\right)\right]_{r_k} \\ & - \frac{1}{(m_k\,s)_{r_k}}\,\frac{1}{r_k\,L_{0\,k}} \sum_{j=1,J}^{m_j \neq m_k} \frac{1}{m_j - m_k} \left(P_{kj}\,L_{kj} - M_{kj}\,N_{kj}\right)_{r_k},\end{aligned} \tag{A77}$$

$$a_{kj} = -\frac{1}{(m_k\,s)_{r_k}} \left(\frac{M_{jk}}{\nu_{L\,k}} + \frac{L_{jk}}{L_{0\,k}}\right)_{r_k}, \tag{A78}$$

$$b_{kj} = -\frac{1}{(m_k\,s)_{r_k}} \left(\frac{N_{jk}}{L_{0\,k}} + \frac{P_{jk}}{\nu_{L\,k}}\right)_{r_k}, \tag{A79}$$

and

$$L_{1\,k} = \lim_{x\to 0}\left(\frac{L_{kk}}{m_k - n\,q}\right) - \frac{r_k\,L_{0\,k}}{x}, \tag{A80}$$

$$P_{1\,k} = \lim_{x\to 0}\left(\frac{P_{kk}}{m_k - n\,q}\right) - \frac{r_k\,P_{0\,k}}{x}, \tag{A81}$$

$$T_{1\,k} = \lim_{x\to 0}\left(\frac{-n\,q\,s}{m_k - n\,q}\right) - \frac{r_k}{x}. \tag{A82}$$

The parameters $A_{S\,k}$ and $A_{L\,k}$ are identified from the numerical solution of the outer equa-

tions in the vicinity of the rational surface by taking the limits

$$\bar{\psi}_{kj} = \psi_j(r_k+\delta) - a_{kj}\,\psi_k(r_k+\delta), \tag{A83}$$

$$\bar{Z}_{kj} = Z_j(r_k+\delta) - b_{kj}\,\psi_k(r_k+\delta), \tag{A84}$$

$$A^{\pm}_{S\,k} = \pm\,\frac{Z_k(r_k\pm|\delta|) - b_{L\,k}\,\psi_k(r_k\pm|\delta|)}{(b_{S\,k}-b_{L\,k})\,|\delta|^{\nu_{S\,k}}} - \frac{[(B_{C\,k}-b_{L\,k}\,A_{C\,k}) + (\gamma_{L\,k}-b_{L\,k}\,\lambda_{L\,k})\,\psi_k(r_k\pm|\delta|)]\,|\delta|}{(b_{S\,k}-b_{L\,k})\,|\delta|^{\nu_{S\,k}}}, \tag{A85}$$

$$A^{\pm}_{L\,k} = \frac{\psi_k(r_k\pm|\delta|) \mp A^{\pm}_{S\,k}|\delta|^{\nu_{S\,k}} \mp A_{C\,k}\,|\delta|}{(1\pm|\delta|\,\lambda_{L\,k})\,|\delta|^{\nu_{L\,k}}} \tag{A86}$$

as $|\delta|\rightarrow 0$. The previous analysis is based on the assumption that

$$0 < D_{I\,k} < 1. \tag{A87}$$

If $D_{I\,k} < 0$ then the indices $\nu_{L\,k}$ and $\nu_{S\,k}$ become complex, indicating that the plasma in the vicinity of the kth rational surface is unstable to ideal interchange modes.[12] On the other hand, if $D_{I\,k} > 1$ then the indices $\nu_{L\,k}$ and $\nu_{S\,k}$ differ by more than 2, and the expansion (A63)–(A66) must consequently be carried out to higher order in $|x|$.

6. Asymptotic Matching Across Rational Surface

Consider the resistive layer solution in the vicinity of the kth rational surface. This solution can be separated into independent tearing and twisting parity components.[2] The even (tearing parity) component is such that $\psi_k(-x) = \psi_k(x)$ throughout the layer, whereas the odd (twisting parity) component is such that $\psi_k(-x) = -\psi_k(x)$. It is helpful to define the quantities

$$A^{e}_{L\,k} = \frac{1}{2}\,(A^{+}_{L\,k} + A^{-}_{L\,k}), \tag{A88}$$

$$A^{o}_{L\,k} = \frac{1}{2}\,(A^{+}_{L\,k} - A^{-}_{L\,k}), \tag{A89}$$

$$A^{e}_{S\,k} = \frac{1}{2}\,(A^{+}_{S\,k} - A^{-}_{S\,k}), \tag{A90}$$

$$A^{o}_{S\,k} = \frac{1}{2}\,(A^{+}_{S\,k} + A^{-}_{S\,k}). \tag{A91}$$

The even and odd layer solutions determine the ratios [2]

$$\Delta^{e}_{k} = r_k^{\nu_{S\,k}-\nu_{L\,k}}\,\frac{2\,A^{e}_{S\,k}}{A^{e}_{L\,k}}, \tag{A92}$$

and

$$\Delta^o_k = r_k^{\nu_{S\,k}-\nu_{L\,k}}\,\frac{2\,A^o_{S\,k}}{A^o_{L\,k}}, \tag{A93}$$

respectively. Moreover, the net toroidal electromagnetic torque acting on the layer can be shown to take the form [7,9]

$$\delta T_k = 2\,n\,\pi^2\left(\frac{\nu_{S\,k}-\nu_{L\,k}}{L_{kk}}\right)_{r_k}\left[|A^e_{L\,k}|^2\,\mathrm{Im}(\Delta^e_k)+|A^o_{L\,k}|^2\,\mathrm{Im}(\Delta^o_k)\right]. \tag{A94}$$

Let

$$\Psi^e_k = r_k^{\nu_{L\,k}}\left(\frac{\nu_{S\,k}-\nu_{L\,k}}{L_{kk}}\right)^{1/2}_{r_k} A^e_{L\,k}, \tag{A95}$$

$$\Delta\Psi^e_k = r_k^{\nu_{S\,k}}\left(\frac{\nu_{S\,k}-\nu_{L\,k}}{L_{kk}}\right)^{1/2}_{r_k} 2\,A^e_{S\,k}, \tag{A96}$$

$$\Psi^o_k = r_k^{\nu_{L\,k}}\left(\frac{\nu_{S\,k}-\nu_{L\,k}}{L_{kk}}\right)^{1/2}_{r_k} A^o_{L\,k}, \tag{A97}$$

$$\Delta\Psi^o_k = r_k^{\nu_{S\,k}}\left(\frac{\nu_{S\,k}-\nu_{L\,k}}{L_{kk}}\right)^{1/2}_{r_k} 2\,A^o_{S\,k}, \tag{A98}$$

The matching conditions become

$$\Delta\Psi^e_k = \Delta^e_k\;\Psi^e_k, \tag{A99}$$

$$\Delta\Psi^o_k = \Delta^o_k\;\Psi^o_k. \tag{A100}$$

Moreover,[7,9]

$$\delta T_k = 2\,n\,\pi^2\,\mathrm{Im}\left(\Psi^{e\,*}_k\,\Delta\Psi^e_k+\Psi^{o\,*}_k\,\Delta\Psi^o_k\right). \tag{A101}$$

7. Toroidal Electromagnetic Torque on Plasma

It follows, from the previous analysis, that the net toroidal electromagnetic torque acting within that equilibrium magnetic flux-surface whose label is r satisfies[7,9]

$$\frac{dT_\phi}{dr} = \sum_{k=1,K}\delta T_k\,\delta(r-r_k), \tag{A102}$$

where

$$\delta T_k = 2\,n\,\pi^2\,\mathrm{Im}\left(\Psi^{e\,*}_k\,\Delta\Psi^e_k+\Psi^{o\,*}_k\,\Delta\Psi^o_k\right). \tag{A103}$$

8. Derivation of Dispersion Relation

Let $\mathbf{y}(r)$ represent the $2J$-dimensional vector of the $\psi_j(r)$ and $Z_j(r)$ functions that satisfy the outer equations, (A47) and (A48).

Suppose that the plasma is surrounded by a close fitting, perfectly conducting wall whose inner surface corresponds to the outermost plasma flux-surface, $r = a$.

Let us launch J linearly independent, well-behaved solution vectors, $\mathbf{y}^e_j(r)$, for $j = 1, J$, from the magnetic axis, $r = 0$, and numerically integrate them to $r = a$. (It is generally necessary to periodically re-orthogonalize the solution vectors to prevent them from becoming collinear. See Ref. 10, Appendix A.3.) The jump conditions imposed at the rational surfaces are

$$\Psi^o_{k'} = 0, \tag{A104}$$

$$\Delta\Psi^e_{k'} = 0, \tag{A105}$$

for $k' = 1, K$.

Next, let us launch a solution vector, $\Delta\mathbf{y}^e_k(r)$, from the kth rational surface, and numerically integrate it to $r = a$. The jump conditions imposed at the rational surfaces are

$$\Psi^o_{k'} = 0, \tag{A106}$$

$$\Delta\Psi^e_{k'} = \delta_{k'k}, \tag{A107}$$

for $k' = 1, K$.

We can form a linear combination of solution vectors,

$$\mathbf{Y}^e_k(r) = \sum_{j=1,J} \alpha^e_{jk}\, \mathbf{y}^e_j + \Delta\mathbf{y}^e_k, \tag{A108}$$

and choose the α^e_{jk} so as to ensure that the physical boundary condition

$$\psi_j(a) = 0, \tag{A109}$$

for $j = 1, J$, is satisfied. By construction, this solution vector is such that

$$\Psi^o_{k'} = 0, \tag{A110}$$

$$\Delta\Psi^e_{k'} = \delta_{k'k}, \tag{A111}$$

for $k' = 1, K$. Let

$$\Psi^e_{k'} = F^{ee}_{k'k}, \tag{A112}$$

$$\Delta\Psi^o_{k'} = F^{oe}_{k'k}, \tag{A113}$$

for $k' = 1, K$. We can associate a $\mathbf{Y}^e_k(r)$ with each rational surface in the plasma.

Let us launch J linearly independent, well-behaved solution vectors, $\mathbf{y}^o_j(r)$, for $j = 1, J$, from the magnetic axis, $r = 0$, and numerically integrate them to $r = a$. The jump conditions imposed at the rational surfaces are

$$\Psi^e_{k'} = 0, \tag{A114}$$

$$\Delta\Psi^o_{k'} = 0, \tag{A115}$$

for $k' = 1, K$.

Next, we can launch a solution vector, $\Delta\mathbf{y}^o_k(r)$, from the kth rational surface, and integrate it to $r = a$. The jump conditions imposed at the rational surfaces are

$$\Psi^e_{k'} = 0, \tag{A116}$$

$$\Delta\Psi^o_{k'} = \delta_{k'k}, \tag{A117}$$

for $k = 1, K$.

We can form the linear combination of solution vectors,

$$\mathbf{Y}^o_k(r) = \sum_{j=1,J} \alpha^o_{jk}\, \mathbf{y}^o_j + \Delta\mathbf{y}^o_k, \tag{A118}$$

and choose the α^o_{jk} so as to satisfy the boundary condition (A125). By construction, this solution vector is such that

$$\Psi^e_{k'} = 0, \tag{A119}$$

$$\Delta\Psi^o_{k'} = \delta_{k'k}, \tag{A120}$$

for $k' = 1, K$. Let

$$\Psi^o_{k'} = F^{oo}_{k'k}, \tag{A121}$$

$$\Delta\Psi^e_{k'} = F^{eo}_{k'k}, \tag{A122}$$

for $k' = 1, K$. We can associate a $\mathbf{Y}^o_k(r)$ with each rational surface in the plasma.

The most general well-behaved solution vector that satisfies the boundary condition (A125) is written

$$\mathbf{Y}(r) = \sum_{k=1,K} (a_k\, \mathbf{Y}^e_k + b_k\, \mathbf{Y}^o_k), \tag{A123}$$

where the a_k and b_k are arbitrary. It follows that

$$\Psi^e_k = \sum_{k'=1,K} F^{ee}_{kk'}\, a_{k'}, \tag{A124}$$

$$\Psi^o_k = \sum_{k'=1,K} F^{oo}_{kk'}\, b_{k'}, \tag{A125}$$

$$\Delta\Psi^e_k = a_k + \sum_{k'=1,K} F^{eo}_{kk'}\, b_{k'}, \tag{A126}$$

$$\Delta\Psi^o_k = b_k + \sum_{k'=1,K} F^{oe}_{kk'}\, a_{k'}, \tag{A127}$$

for $k = 1, K$. Let $\mathbf{\Psi}^e$, $\mathbf{\Psi}^o$, $\mathbf{\Delta\Psi}^e$, and $\mathbf{\Delta\Psi}^o$ be the $K \times 1$ vectors of the Ψ^e_k, Ψ^o_k, $\Delta\Psi^e_k$, and $\Delta\Psi^o_k$ values, respectively. Let $\mathbf{F}^{ee}$, $\mathbf{F}^{eo}$, $\mathbf{F}^{oe}$, and $\mathbf{F}^{oo}$ be the $K \times K$ matrices of the $F^{ee}_{kk'}$, $F^{eo}_{kk'}$, $F^{oe}_{kk'}$, and $F^{oo}_{kk'}$ values, respectively. Equations (A140)–(A143) can be combined to give the dispersion relation

$$\begin{pmatrix} \mathbf{\Delta\Psi}^e \\ \mathbf{\Delta\Psi}^o \end{pmatrix} = \begin{pmatrix} \mathbf{E}^e & \mathbf{\Gamma} \\ \mathbf{\Gamma}' & \mathbf{E}^o \end{pmatrix} \begin{pmatrix} \mathbf{\Psi}^e \\ \mathbf{\Psi}^o \end{pmatrix}, \tag{A128}$$

where

$$\mathbf{E}^e = (\mathbf{F}^{ee})^{-1}, \tag{A129}$$

$$\mathbf{E}^o = (\mathbf{F}^{oo})^{-1}, \tag{A130}$$

$$\mathbf{\Gamma} = \mathbf{F}^{eo}\, \mathbf{E}^o, \tag{A131}$$

$$\mathbf{\Gamma}' = \mathbf{F}^{oe}\, \mathbf{E}^e. \tag{A132}$$

Now, according to Eqs. (A61) and (A125),

$$T_\phi(a) = 0. \tag{A133}$$

In other words, the net toroidal electromagnetic torque acting on the plasma is zero. Hence, it follows from Eqs. (A118) and (A119) that

$$\mathbf{\Psi}^{e\,\dagger}\, \mathbf{\Delta\Psi}^e - \mathbf{\Delta\Psi}^{e\,\dagger}\, \mathbf{\Psi}^e + \mathbf{\Psi}^{o\,\dagger}\, \mathbf{\Delta\Psi}^o - \mathbf{\Delta\Psi}^{o\,\dagger}\, \mathbf{\Psi}^o = 0. \tag{A134}$$

Thus, making use of the dispersion relation (A144), we deduce that[4,5,7,9]

$$\mathbf{E}^{e\,\dagger} = \mathbf{E}^{e}, \tag{A135}$$

$$\mathbf{E}^{o\,\dagger} = \mathbf{E}^{o}, \tag{A136}$$

$$\mathbf{\Gamma}' = \mathbf{\Gamma}^{\dagger}. \tag{A137}$$

Thus, the dispersion relation can be written[3–5,7]

$$\begin{pmatrix} \mathbf{E}^e - \mathbf{\Delta}^e & \mathbf{\Gamma} \\ \mathbf{\Gamma}' & \mathbf{E}^o - \mathbf{\Delta}^o \end{pmatrix} \begin{pmatrix} \mathbf{\Psi}^e \\ \mathbf{\Psi}^o \end{pmatrix} = \begin{pmatrix} \mathbf{0} \\ \mathbf{0} \end{pmatrix}, \tag{A138}$$

where $\mathbf{\Delta}^e$ and $\mathbf{\Delta}^o$ are the diagonal $K \times K$ matrices of the Δ^e_k and Δ^o_k values, respectively. Note that, according to Eqs. (A151)–(A153), the $\mathbf{E}^e$ and $\mathbf{E}^o$ matrices are Hermitian, and the $\mathbf{\Gamma}'$ matrix is the Hermitian conjugate of the $\mathbf{\Gamma}$ matrix.

Appendix B: Solution of Linearized Resistive-MHD Layer Equations

1. Basic Equations

Let us assume that all perturbed quantities vary in time as $\exp(\gamma\, t)$, where γ is the complex growth-rate of the instability. The linearized, resistive-MHD equations that govern perturbed quantities in the inner region are [2]

$$\delta\mathbf{B} = \nabla \times (\boldsymbol{\xi} \times \mathbf{B}) - \frac{\eta}{\gamma'}\, \nabla \times \delta\mathbf{J}, \tag{B1}$$

$$\nabla \delta P = \delta\mathbf{J} \times \mathbf{B} + \mathbf{J} \times \delta\mathbf{B} - \rho\, \gamma'^{\,2}\, \boldsymbol{\xi}, \tag{B2}$$

$$\delta\mathbf{J} = \nabla \times \delta\mathbf{B}, \tag{B3}$$

$$\delta P = -\boldsymbol{\xi} \cdot \nabla P - \mathit{\Gamma}\, P\, \nabla \cdot \boldsymbol{\xi}. \tag{B4}$$

Here,

$$\gamma'(r) = \gamma - \mathrm{i}\, n\, \Omega_\phi(r), \tag{B5}$$

where $\Omega_\phi(r)$ is the plasma toroidal angular velocity. (We are neglecting the effect of velocity shear in the preceding equations.) Moreover, $\eta(r)$ and $\rho(r)$ are the plasma resistivity and density profiles, respectively. Finally, $\mathit{\Gamma} = 5/3$ is the plasma ratio of specific heats.

2. Layer Equations

Consider the segment of the inner region centered on the kth rational surface. It is helpful to define

$$a_0(r) = \left\langle R^2 \right\rangle, \tag{B6}$$

$$c_0(r) = \left\langle |\nabla r|^{-2} \right\rangle, \tag{B7}$$

$$d_0(r) = \left\langle |\nabla r|^{-2} R^2 \right\rangle, \tag{B8}$$

$$e_0(r) = \left\langle |\nabla r|^{-2} R^4 \right\rangle, \tag{B9}$$

$$x_0(r) = \langle |\nabla r|^2 \rangle, \tag{B10}$$

$$y_0(r) = \left\langle R^4 \right\rangle, \tag{B11}$$

as well as

$$F_R(r) = \frac{1 + x_0\,\alpha_\epsilon/q^2}{c_0 + \alpha_\epsilon/q^2}, \tag{B12}$$

$$F_A(r) = \frac{y_0\,(1 + x_0\,\alpha_\epsilon/q^2) - a_0^2}{f^{\,2}\,F_R}, \tag{B13}$$

and

$$\omega_H(r) = \frac{B_0}{R_0}\,\frac{n\,s}{\sqrt{\mu_0\,\rho\,F_A}}, \tag{B14}$$

$$\omega_\eta(r) = \frac{\eta\,F_R}{\mu_0\,r^2}, \tag{B15}$$

$$L(r) = \frac{\omega_A}{\omega_\eta}. \tag{B16}$$

It is assumed that $L \gg 1$.

In the vicinity of the kth rational surface, Eqs. (B1)–(B4) can be shown to reduce to [2]

$$0 = \frac{d^2\Psi}{dX^2} - H_k\,\frac{d\Upsilon}{dX} - Q_k\,(\Psi - X\,\Xi), \tag{B17}$$

$$0 = Q_k^2\,\frac{d^2\Xi}{dX^2} - Q_k\,X^{\,2}\,\Xi + E_k\,\Upsilon + Q_k\,X\,\Psi + \Lambda, \tag{B18}$$

$$0 = Q_k\,\frac{d^2\Upsilon}{dX^2} - X^{\,2}\,\Upsilon - G_k\,Q_k^2\,\Upsilon + (G_k - K_k\,E_k)\,Q_k^2\,\Xi + X\,\Psi - K_k\,Q_k^2\,\Lambda, \tag{B19}$$

$$0 = H_k\,\frac{d^2\Lambda}{dX^2} - \frac{d\Lambda}{dX} + F_k\,\frac{d\Upsilon}{dX}. \tag{B20}$$

Here,

$$x = r - r_k, \tag{B21}$$

$$\Psi(x) = \psi_k(x), \tag{B22}$$

$$X = \left(L^{1/3}\, \frac{x}{r} \right)_{r_k}, \tag{B23}$$

$$Q_k = \left(L^{1/3}\, \frac{\gamma'}{\omega_H} \right)_{r_k}, \tag{B24}$$

and

$$E_k = \left[\frac{\alpha_p}{s^2} \left\{ (c_0 + \alpha_\epsilon/q^2) \left(-r\, \frac{da_0}{dr} + a_0\, \alpha_f \right) + \frac{a_0\, s}{F_R} \right\} \right]_{r_k}, \tag{B25}$$

$$F_k = \left[\frac{\alpha_p^2}{s^2} \left([c_0 + \alpha_\epsilon/q^2]\, e_0 - d_0^2 \right) \right]_{r_k}, \tag{B26}$$

$$G_k = \left[\frac{a_0\, (c_0 + \alpha_\epsilon/q^2)}{\Gamma\, P}\, \frac{F_R}{F_A} \right]_{r_k}, \tag{B27}$$

$$H_k = \left[\frac{\alpha_p}{s} \left(d_0 - \frac{a_0}{F_R} \right) \right]_{r_k}, \tag{B28}$$

$$K_k = \left[\frac{s^2}{\alpha_p^2\, f^{\,2}}\, \frac{F_R}{F_A} \right]_{r_k}. \tag{B29}$$

Let us write

$$\Psi(X) = \Psi^e(X) + \Psi^o(X) + A_0\, X, \tag{B30}$$

$$\Xi(X) = \Xi^e(X) + \Xi^o(X) + A_0, \tag{B31}$$

$$\Upsilon(X) = \Upsilon^e(X) + \Upsilon^o(X) + A_0, \tag{B32}$$

$$\Lambda(X) = \Lambda^e(X) + \Lambda^o(X) - A_0\, E_k, \tag{B33}$$

where A_0 is an arbitrary constant, and $\Psi^e(-X) = \Psi^e(X)$, $\Psi^o(-X) = -\Psi^o(X)$, etc. Equations (B17)–(B20) can be shown to separate into the following two independent sets of equations:[2]

$$0 = \frac{d^2\Psi^{e,o}}{dX^2} - H_k\, \frac{d\Upsilon^{o,e}}{dX} - Q_k\, (\Psi^{e,o} - X\, \Xi^{o,e}), \tag{B34}$$

$$0 = Q_k^2\, \frac{d^2\Xi^{o,e}}{dX^{\,2}} - Q_k\, X^{\,2}\, \Xi^{o,e} + (E_k + F_k)\, \Upsilon^{o,e} + Q_k\, X\, \Psi^{e,o} + H_k\, \frac{d\Psi^{e,o}}{dX}, \tag{B35}$$

$$\begin{aligned} 0 = {} & Q_k\, \frac{d^2\Upsilon^{o,e}}{dX^{\,2}} - X^{\,2}\, \Upsilon^{o,e} - Q_k^2\, (G_k + K_k\, F_k)\, \Upsilon^{o,e} + Q_k^2\, (G_k - K_k\, E_k)\, \Xi^{o,e} \\ & - Q_k^2\, K_k\, H_k\, \frac{d\Psi^{e,o}}{dX}, \end{aligned} \tag{B36}$$

where

$$\Lambda^{o,e} = H_k \frac{d\Psi^{e,o}}{dX} + F_k \Upsilon^{o,e}. \tag{B37}$$

The first set (involving Ψ^e) governs tearing parity layer solutions, whereas the second (involving Ψ^o) governs twisting parity solutions.

3. Asymptotic Matching

In the limit $|X| \rightarrow \infty$, the asymptotic behavior of the well-behaved solutions of the layer equations, (B34)–(B37), is such that

$$\Psi^e(X) \rightarrow a^e_L \, |X|^{\nu_{L\,k}} + a^e_S \, |X|^{\nu_{S\,k}}, \tag{B38}$$

$$\Psi^o(X) \rightarrow \mathrm{sgn}(X) \, (a^o_L \, |X|^{\nu_{L\,k}} + a^o_S \, |X|^{\nu_{S\,k}}) \, . \tag{B39}$$

These solutions are undetermined to an arbitrary multiplicative constant, which means that the ratios a^e_S/a^e_L and a^o_S/a^o_L are fully determined. Here,

$$\nu_{L\,k} = -\frac{1}{2} - \sqrt{D_{I\,k}}, \tag{B40}$$

$$\nu_{S\,k} = -\frac{1}{2} + \sqrt{D_{I\,k}}, \tag{B41}$$

where

$$D_{I\,k} = \frac{1}{4} - E_k - F_k - H_k. \tag{B42}$$

The parameter $D_{I\,k}$ can be shown to be identical to the corresponding parameter defined in Section A 5. Asymptotic matching to the ideal-MHD solution in the outer region yields

$$\Delta^e_k = L_k^{(\nu_{L\,k} - \nu_{L\,k})/3} \, \hat{\Delta}^e_k, \tag{B43}$$

$$\Delta^o_k = L_k^{(\nu_{L\,k} - \nu_{L\,k})/3} \, \hat{\Delta}^o_k, \tag{B44}$$

where $L_k = L(r_k)$, and

$$\hat{\Delta}^e_k = \frac{2\,a^e_S}{a^e_L}, \tag{B45}$$

$$\hat{\Delta}^o_k = \frac{2\,a^o_S}{a^o_L}. \tag{B46}$$

The hydromagnetic frequency, resistive diffusion rate, and Lundquist number of the plasma are defined

$$\omega_A(r) = \frac{B_0}{R_0}\,\frac{1}{\sqrt{\mu_0\,\rho}}, \tag{B47}$$

$$\omega_R(r) = \frac{\eta}{\mu_0\,\bar{a}^{\,2}}, \tag{B48}$$

$$S(r) = \frac{\omega_A}{\omega_R}, \tag{B49}$$

respectively. Here, the plasma minor radius, $\bar{a}$, is specified in Sect. III. It follows that

$$S = f_S\,L \tag{B50}$$

$$\omega_A = f_A\,\omega_H, \tag{B51}$$

where

$$f_S(r) = \frac{F_A^{\,1/2}\,F_R}{n\,s}\,\frac{\bar{a}^{\,2}}{r^2}, \tag{B52}$$

$$f_A(r) = \frac{n\,s}{F_A^{\,1/2}}. \tag{B53}$$

Thus, we can write

$$\Delta_k^e = S_k^{(2/3)\sqrt{D_{I\,k}}}\,\tilde{\Delta}_k^e(\tilde{Q}_k, E_k + F_k, H_k, K_k\,E_k - G_k, K_k\,F_k + G_k, K_k\,H_k, f_{A\,k}, f_{S\,k}), \tag{B54}$$

$$\Delta_k^o = S_k^{(2/3)\sqrt{D_{I\,k}}}\,\tilde{\Delta}_k^o(\tilde{Q}_k, E_k + F_k, H_k, K_k\,E_k - G_k, K_k\,F_k + G_k, K_k\,H_k, f_{A\,k}, f_{S\,k}), \tag{B55}$$

where

$$\gamma = \mathrm{i}\,n\,\Omega_k + \frac{\tilde{Q}_k}{S_k^{\,1/3}}\,\omega_{A\,k}, \tag{B56}$$

and

$$\tilde{Q}_k = \left(\frac{f_{S\,k}^{\,1/3}}{f_{A\,k}}\right) Q_k, \tag{B57}$$

$$\tilde{\Delta}_k^{e,o} = \frac{\hat{\Delta}_k^{e,o}}{f_{S\,k}^{(2/3)\sqrt{D_{I\,k}}}}. \tag{B58}$$

Here, $S_k = S(r_k)$, $\Omega_k = \Omega(r_k)$, $\omega_{A\,k} = \omega_A(r_k)$, $f_{A\,k} = f_A(r_k)$, and $f_{S\,k} = f_S(r_k)$.

k	$E_k + F_k$	H_k	$K_k\,E_k - G_k$	$K_k\,F_k + G_k$	$K_k\,H_k$	$D_{I\,k}$	$f_{A\,k}$	$f_{S\,k}$
2	−0.04765	0.01815	−52.20	50.21	0.7597	0.2795	0.6409	1.478
2	−0.01263	0.005102	−339.3	331.3	3.207	0.2575	0.8904	0.6181

TABLE I. Resonant layer parameters for a plasma equilibrium characterized by $\bar{a} = 0.3$, $\kappa = 1.8$, $\delta = 0.25$, $q_0 = 1.05$, $q_a = 3.95$, and $\beta_N = 1.0$.

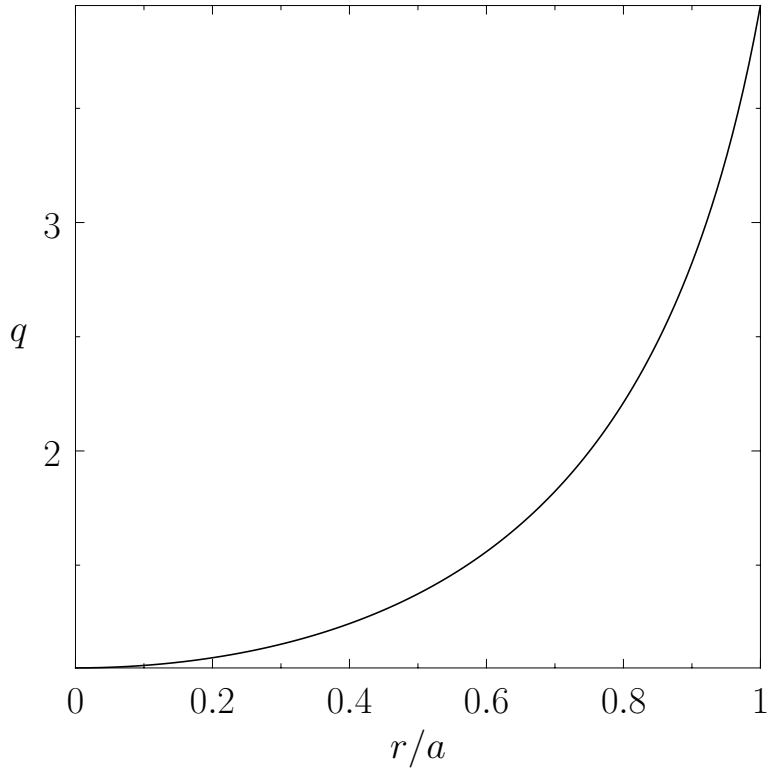

FIG. 1. Safety-factor profile for a plasma equilibrium characterized by $\bar{a} = 0.3$, $\kappa = 1.8$, $\delta = 0.25$, $q_0 = 1.05$, $q_a = 3.95$, and $\beta_N = 1.0$.

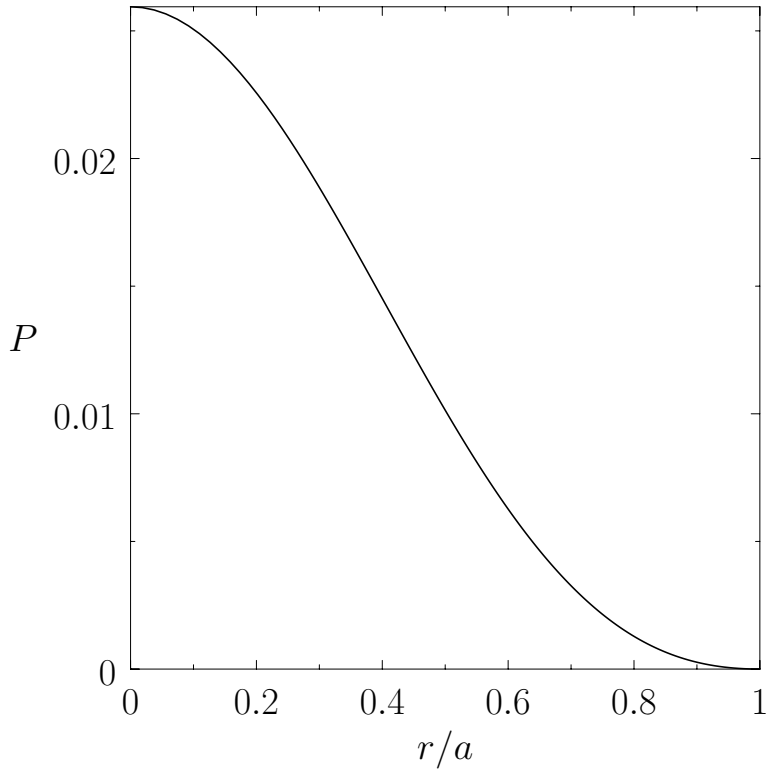

FIG. 2. Pressure profile for a plasma equilibrium characterized by $\bar{a} = 0.3$, $\kappa = 1.8$, $\delta = 0.25$, $q_0 = 1.05$, $q_a = 3.95$, and $\beta_N = 1.0$.

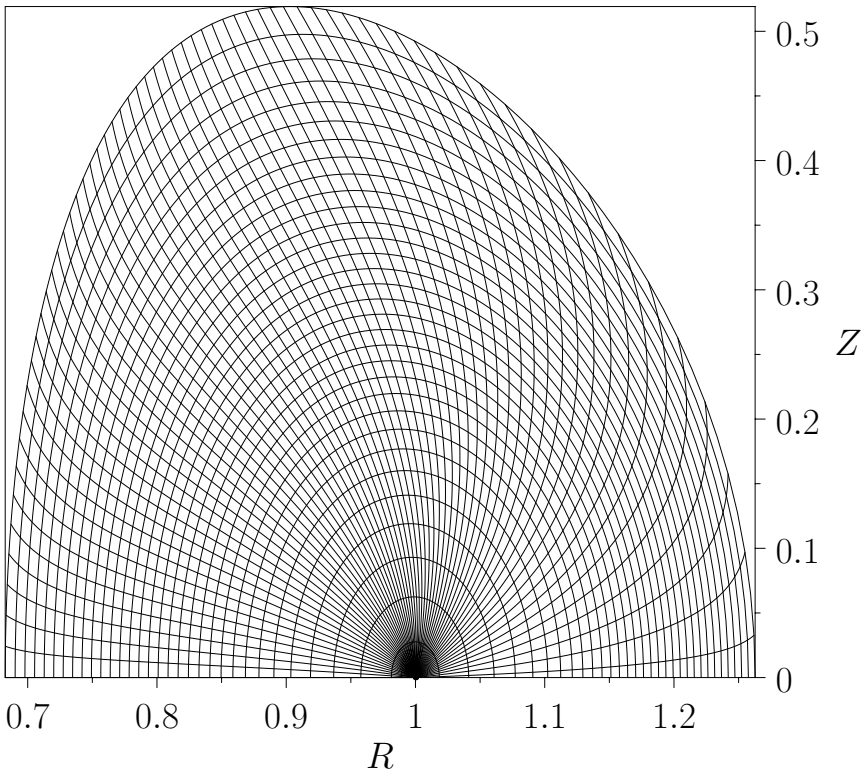

FIG. 3. Flux coordinate system for a plasma equilibrium characterized by $\bar{a} = 0.3$, $\kappa = 1.8$, $\delta = 0.25$, $q_0 = 1.05$, $q_a = 3.95$, and $\beta_N = 1.0$. The curves show contours of the flux-surface label r, and the straight poloidal angle θ.

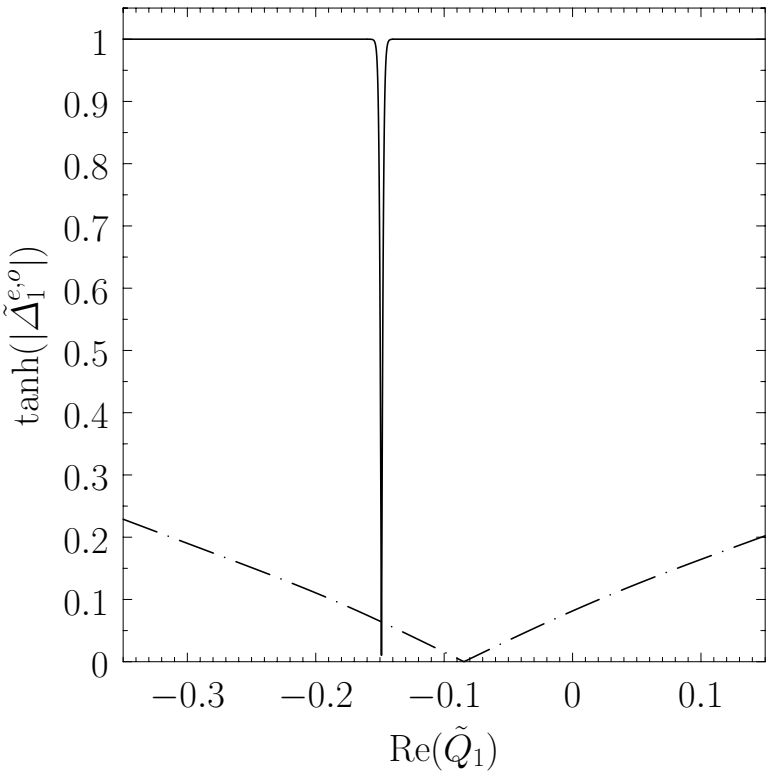

FIG. 4. Normalized $n = 1$ layer stability parameters at the $q = 2$ surface, calculated with the resonant layer parameters specified in Table I as functions of the real part of the normalized growth-rate. The dashed curve shows $|\tilde{\Delta}_1^e|$ calculated with $\mathrm{Im}(\tilde{Q}_1) = \pm 1.465 \times 10^{-1}$. The solid curve shows $|\tilde{\Delta}_1^o|$ calculated with $\mathrm{Im}(\tilde{Q}_1) = \pm 2.578 \times 10^{-1}$.

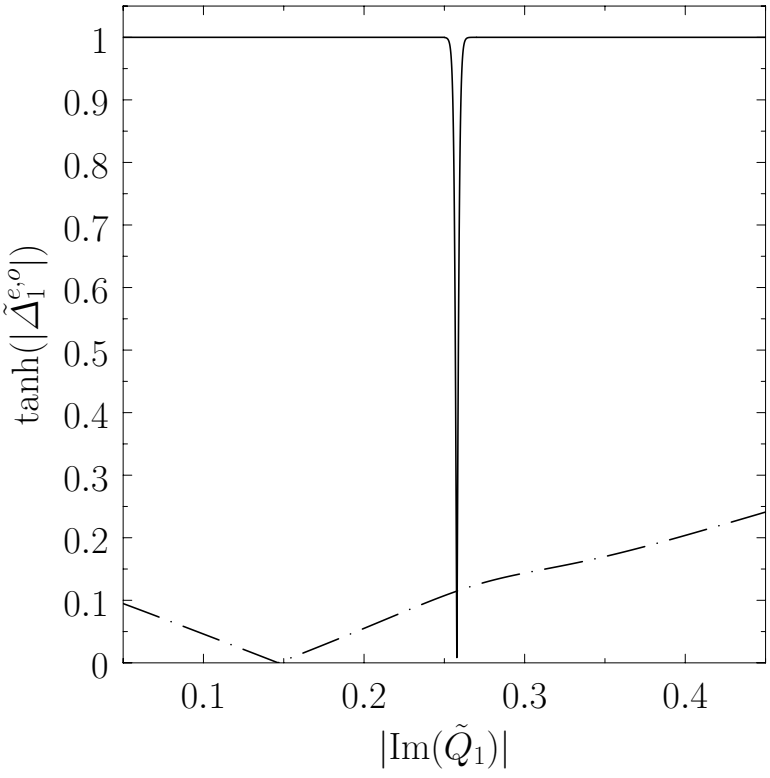

FIG. 5. Normalized $n = 1$ layer stability parameters at the $q = 2$ surface, calculated with the resonant layer parameters specified in Table I as functions of the imaginary part of the normalized growth-rate. The dashed curve shows $|\tilde{\Delta}_1^e|$ calculated with $\mathrm{Re}(\tilde{Q}_1) = -8.458 \times 10^{-2}$. The solid curve shows $|\tilde{\Delta}_1^o|$ calculated with $\mathrm{Re}(\tilde{Q}_1) = -1.488 \times 10^{-1}$.

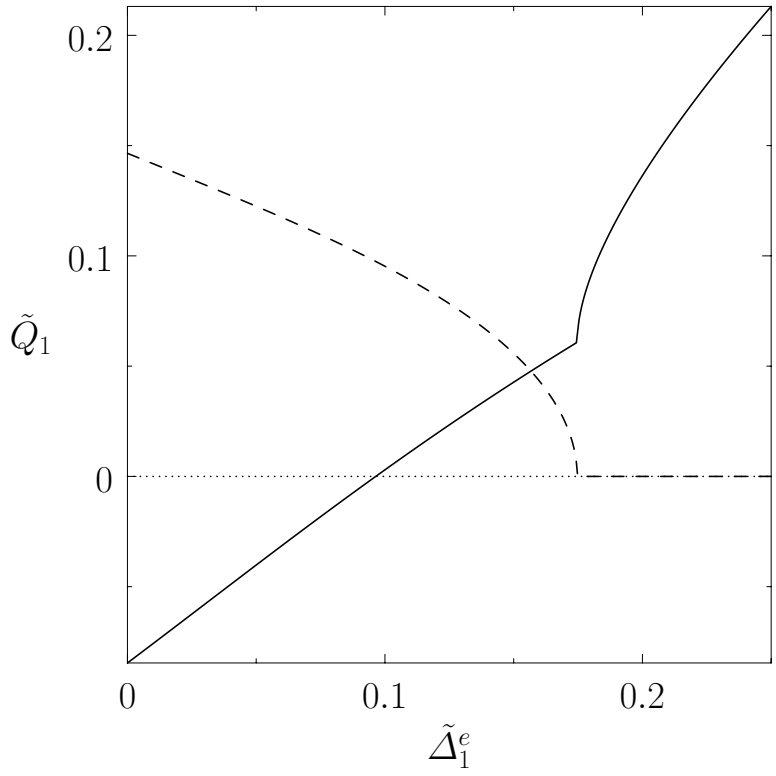

FIG. 6. Normalized $n = 1$ growth-rate of the tearing parity mode at the $q = 2$ surface, calculated with the resonant layer parameters listed in Table I as a function of the real part of the normalized tearing parity layer stability parameter. The solid curve shows $\mathrm{Re}(\tilde{Q}_1)$, and the dashed curve shows $\mathrm{Im}(\tilde{Q}_1)$. The imaginary part of $\tilde{\Delta}_1^e$ is zero.

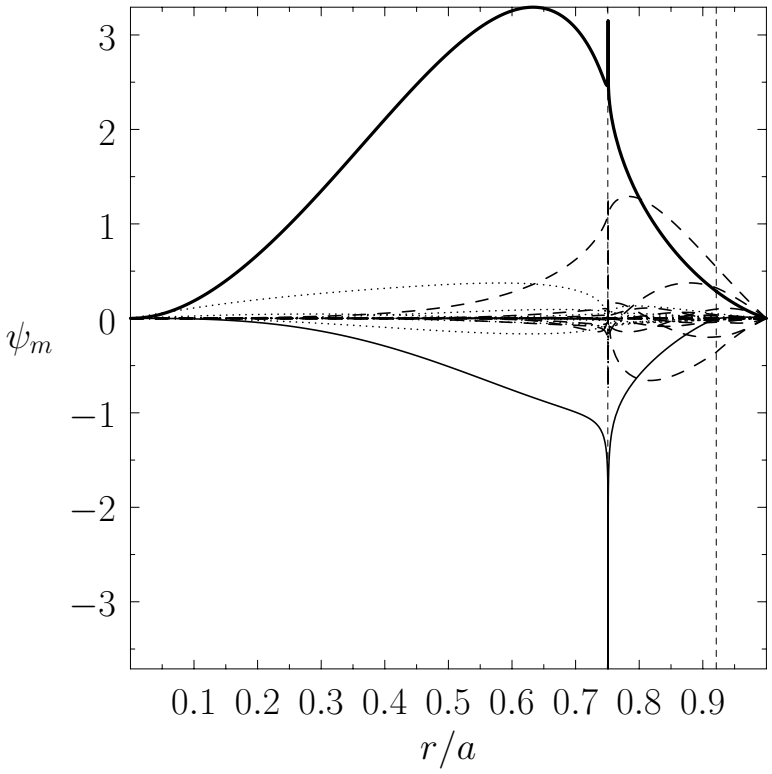

FIG. 7. Eigenfunction of the $n = 1$ tearing parity mode that only reconnects magnetic flux at the $q = 2$ surface. The thicker solid black curve shows the resonant $m = 2$ harmonic. The thiner solid black curve shows the resonant $m = 3$ harmonic. The dotted curves show non-resonant harmonics whose poloidal mode numbers are less than 2. The dashed curves show non-resonant harmonics whose poloidal mode numbers are greater than 3. The vertical dashed lines indicate the locations of the $q = 2$ and $q = 3$ surfaces.